

Review

Recent Advances in Dendrite Suppression Strategies for Solid-State Lithium Batteries: From Interface Engineering to Material Innovations

Abniel Machín ^{1,*}, Francisco Díaz ², María C. Cotto ², José Ducongé ² and Francisco Márquez ^{2,*}

¹ Environmental Catalysis Research Lab, Division of Science, Technology and Environment, Cupey Campus, Universidad Ana G. Méndez, Cupey, PR 00926, USA

² Nanomaterials Research Group, Department of Natural Sciences and Technology, Division of Natural Sciences, Technology and Environment, Universidad Ana G. Méndez-Gurabo Campus, Gurabo, PR 00778, USA; fdiaz@uagm.edu (F.D.); mcotto48@uagm.edu (M.C.C.); jduconge@uagm.edu (J.D.)

* Correspondence: machina1@uagm.edu (A.M.); fmarquez@uagm.edu (F.M.); Tel.: +1-787-878-2612 (ext. 220) (A.M.); +1-787-743-7979 (ext. 4250) (F.M.)

Abstract

Solid-state lithium batteries (SSLBs) have emerged as a promising alternative to conventional lithium-ion systems due to their superior safety profile, higher energy density, and potential compatibility with lithium metal anodes. However, a major challenge hindering their widespread deployment is the formation and growth of lithium dendrites, which compromise both performance and safety. This review provides a comprehensive and structured overview of recent advances in dendrite suppression strategies, with special emphasis on the role played by the nature of the solid electrolyte. In particular, we examine suppression mechanisms and material innovations within the three main classes of solid electrolytes: sulfide-based, oxide-based, and polymer-based systems. Each electrolyte class presents distinct advantages and challenges in relation to dendrite behavior. Sulfide electrolytes, known for their high ionic conductivity and good interfacial wettability, suffer from poor mechanical strength and chemical instability. Oxide electrolytes exhibit excellent electrochemical stability and mechanical rigidity but often face high interfacial resistance. Polymer electrolytes, while mechanically flexible and easy to process, generally have lower ionic conductivity and limited thermal stability. This review discusses how these intrinsic properties influence dendrite nucleation and propagation, including the role of interfacial stress, grain boundaries, void formation, and electrochemical heterogeneity. To mitigate dendrite formation, we explore a variety of strategies including interfacial engineering (e.g., the use of artificial interlayers, surface coatings, and chemical additives), mechanical reinforcement (e.g., incorporation of nanostructured or gradient architectures, pressure modulation, and self-healing materials), and modifications of the solid electrolyte and electrode structure. Additionally, we highlight the critical role of advanced characterization techniques—such as in situ electron microscopy, synchrotron-based X-ray diffraction, vibrational spectroscopy, and nuclear magnetic resonance (NMR)—for elucidating dendrite formation mechanisms and evaluating the effectiveness of suppression strategies in real time. By integrating recent experimental and theoretical insights across multiple disciplines, this review identifies key limitations in current approaches and outlines emerging research directions. These include the design of multifunctional interphases, hybrid electrolytes, and real-time diagnostic tools aimed at enabling the development of reliable, scalable, and dendrite-free SSLBs suitable for practical applications in next-generation energy storage.



Academic Editors: Changmin Shi and Mingpeng Yu

Received: 25 June 2025

Revised: 5 August 2025

Accepted: 7 August 2025

Published: 8 August 2025

Citation: Machín, A.; Díaz, F.; Cotto, M.C.; Ducongé, J.; Márquez, F. Recent Advances in Dendrite Suppression Strategies for Solid-State Lithium Batteries: From Interface Engineering to Material Innovations. *Batteries* **2025**, *11*, 304. <https://doi.org/10.3390/batteries11080304>

Copyright: © 2025 by the authors. Licensee MDPI, Basel, Switzerland. This article is an open access article distributed under the terms and conditions of the Creative Commons Attribution (CC BY) license (<https://creativecommons.org/licenses/by/4.0/>).

Keywords: solid-state lithium batteries; lithium dendrites; solid electrolytes; interface engineering; interlayers; coatings; composite electrolytes; mechanical design; advanced characterization

1. Introduction

Solid-state lithium batteries (SSLBs) are increasingly considered a transformative platform in energy storage, offering a route to overcome the intrinsic limitations of conventional lithium-ion batteries (LIBs). The fundamental innovation of SSLBs lies in the replacement of flammable organic liquid electrolytes with solid-state ionic conductors. This architectural shift addresses key safety concerns such as leakage, volatility, and thermal runaway, while enabling the use of lithium metal as an anode, an element with the highest known theoretical specific capacity ($3860 \text{ mAh}\cdot\text{g}^{-1}$), and the lowest electrochemical potential among all metals (-3.04 V vs. SHE), which together unlock the possibility of achieving gravimetric energy densities exceeding $500 \text{ Wh}\cdot\text{kg}^{-1}$ [1,2]. The structure of SSLBs resembles that of conventional LIBs but introduces significant differences in materials and interfacial behavior. A typical SSLB consists of a lithium metal anode, a solid-state electrolyte (SSE), and a high-voltage cathode such as $\text{LiNi}_{0.8}\text{Co}_{0.1}\text{Mn}_{0.1}\text{O}_2$ (NCM811) or LiCoO_2 . The SSE is required to exhibit high lithium-ion conductivity ($\geq 10^{-3} \text{ S}\cdot\text{cm}^{-1}$), negligible electronic conductivity, and robust mechanical properties to simultaneously ensure ion transport and block dendrite growth [3]. However, combining these properties in a single material remains a complex challenge, leading to the exploration of diverse classes of SSEs including ceramics, sulfides, polymers, and hybrid composites [4].

Oxide-based electrolytes such as garnet-type $\text{Li}_7\text{La}_3\text{Zr}_2\text{O}_{12}$ (LLZO) exhibit excellent stability against lithium and wide electrochemical windows ($>5 \text{ V}$), but their high interfacial resistance and brittleness pose practical limitations [5]. Sulfide-based electrolytes such as $\text{Li}_{10}\text{GeP}_2\text{S}_{12}$ [6] and $\text{Li}_6\text{PS}_5\text{Cl}$ [7] offer exceptional room-temperature ionic conductivities ($>10^{-2} \text{ S}\cdot\text{cm}^{-1}$) and softness, promoting better interfacial contact. However, they are highly sensitive to air and moisture, releasing toxic H_2S gas upon degradation [4]. Polymeric electrolytes, particularly polyethylene oxide (PEO) with LiTFSI [8], are flexible and easier to process but suffer from poor ionic conductivity at room temperature and limited electrochemical stability [9].

To harness the advantages of multiple classes, researchers have proposed composite electrolytes that incorporate ceramic fillers into polymer matrices, aiming to combine mechanical flexibility with enhanced conductivity. While promising, these systems still face challenges related to phase compatibility, homogeneity, and interfacial degradation [10]. One of the most significant bottlenecks in SSLB development is the engineering of the solid–solid interfaces. Unlike liquid electrolytes, which wet electrode surfaces and reduce interfacial resistance naturally, SSEs require careful interfacial tuning. Poor contact at interfaces can result in high impedance, void formation, and localized current densities that exacerbate dendrite growth. Methods such as interlayer coatings (e.g., Li_3PO_4 , LiNbO_3), hot pressing, and surface modification are actively being pursued to mitigate these issues [11]. Moreover, the SSE must serve as both an efficient lithium-ion conductor and a mechanical barrier against dendrite penetration. While ceramics provide the required mechanical strength, they are brittle and susceptible to microcracking. Polymers, though more compliant, may deform under cycling-induced stress. Thus, optimizing the mechanical profile of SSEs is as critical as enhancing their ionic properties [12]. Industrially, SSLBs are drawing strong interest from companies like QuantumScape, Toyota, and Solid Power. Prototypes have shown energy densities above $400 \text{ Wh}\cdot\text{kg}^{-1}$, fast-charging capabilities, and extended cycle life, though full validation under practical conditions remains pending.

Toyota, for example, has publicly announced its roadmap toward commercial SSLBs before 2030 [13].

Despite these advances, critical challenges persist, including cost-effective synthesis, ambient stability of materials, scalable fabrication techniques, and, most importantly, dendrite suppression. Understanding the mechanisms that govern dendrite formation and propagation through solid electrolytes is crucial to unlocking the full potential of SSLBs. These interfacial and mechanical challenges form the scientific basis for the current review.

2. Understanding Lithium Dendrites in Solid-State Lithium Batteries (SSLBs)

2.1. Mechanism of Dendrite Formation

Lithium dendrite formation remains a critical challenge in the development of solid-state lithium batteries (SSLBs), undermining their potential advantages in energy density and safety [14]. The formation of dendrites involves complex interplays between electrochemical, mechanical, and structural factors within the battery system [15]. Recent studies have elucidated that lithium dendrites can initiate at the interface between the lithium metal anode and the solid electrolyte, particularly at sites of inhomogeneous current distribution or mechanical defects. For instance, molecular dynamics simulations have demonstrated that lithium deposition leads to the accumulation of internal stress, culminating in the fracture of the solid electrolyte at dendrite tips. This fracture facilitates the propagation of dendrites through the electrolyte, compromising the battery's integrity [16,17]. Furthermore, the microstructural characteristics of the solid electrolyte, such as grain boundaries in polycrystalline materials, play a significant role in dendrite formation. Dendrite nuclei within grains tend to deflect towards and propagate along grain boundaries, where fractures exhibit mixed-mode patterns contingent on fracture toughness and the angle between dendrites and grain boundaries [16]. In addition to mechanical factors, electrochemical conditions at the electrode-electrolyte interface influence dendrite initiation. Poor interfacial contact can lead to high polarization voltage during lithium dissolution, increasing the likelihood of dendrite formation in subsequent deposition steps. Moreover, the presence of crystalline defects and dislocations near dendrite tips has been observed, suggesting that these structural irregularities serve as pathways for lithium insertion and dendrite growth [18,19].

2.2. Impact on Battery Performance and Safety

The propagation of lithium dendrites through solid electrolytes poses a significant threat to the performance and safety of SSLBs. Once initiated, dendrites can penetrate the solid electrolyte, leading to internal short circuits that result in rapid capacity loss and potential thermal runaway [6]. This phenomenon has been observed in various solid electrolyte systems, including garnet-type and sulfide-based electrolytes. Advanced characterization techniques, such as operando optical microscopy and ex situ dark-field X-ray microscopy, have provided insights into the strain patterns and lattice orientation changes associated with dendrite growth. These studies have revealed that dendrite-induced fractures often originate at grain boundaries and are accompanied by the formation of dislocations anchored to dendrite tips [20]. Moreover, nuclear magnetic resonance (NMR) and magnetic resonance imaging (MRI) studies have identified two distinct mechanisms of dendrite formation in solid-state batteries: non-uniform lithium plating at electrode-electrolyte interfaces and local lithium-ion reduction at grain boundaries. These mechanisms contribute to the complex interplay between electrochemical and mechanical factors driving dendrite propagation [19].

The presence of lithium dendrites severely compromises the reliability of SSLBs. Dendrite-induced short circuits can lead to catastrophic battery failure, posing safety hazards such as fires or explosions [21,22]. Additionally, dendrite growth increases the internal resistance of the battery, reducing its efficiency and life cycle [23]. To mitigate these risks, various strategies have been proposed, including the development of solid electrolytes with enhanced mechanical properties, engineering of electrode-electrolyte interfaces to promote uniform lithium deposition, and the application of pulse-current protocols to suppress dendrite formation [24,25]. Despite these efforts, achieving long-term dendrite suppression remains a significant challenge, requiring further research into the fundamental mechanisms governing dendrite growth and propagation [26].

3. Dendrite Suppression Strategies

3.1. Material Innovations

The suppression of lithium dendrite formation is paramount for the advancement of SSLBs. Material innovations, particularly in the development of advanced solid electrolytes, play a crucial role in mitigating dendritic growth. These electrolytes can be broadly categorized into sulfide-based, oxide-based, and polymer-based electrolytes, each offering unique advantages and challenges.

3.1.1. Sulfide-Based Electrolytes

Sulfide-based solid electrolytes are renowned for their exceptionally high lithium-ion conductivities, often surpassing those of conventional liquid electrolytes. Among these, lithium germanium phosphorous sulfide ($\text{Li}_{10}\text{GeP}_2\text{S}_{12}$ or LGPS) stands out, exhibiting ionic conductivities exceeding $10 \text{ mS}\cdot\text{cm}^{-1}$ at room temperature [27]. This remarkable conductivity is attributed to its unique crystal structure, which facilitates rapid lithium-ion transport through interconnected pathways. The high ionic conductivity of sulfide electrolytes like LGPS enables fast charge–discharge rates and improved power densities in solid-state lithium batteries (SSLBs) [28]. Additionally, the soft mechanical nature of sulfide electrolytes allows for better contact with electrode materials, reducing interfacial resistance and enhancing overall battery performance [29]. Despite their superior ionic conductivities, sulfide-based electrolytes face challenges related to mechanical properties and chemical stability. They are generally softer and more prone to deformation under pressure, which can compromise the structural integrity of the battery [30]. Moreover, their sensitivity to moisture and oxygen necessitates stringent handling conditions to prevent degradation and the release of toxic hydrogen sulfide gas. To address these issues, composite approaches have been explored. Incorporating polymers as binders or frameworks within sulfide electrolytes can enhance flexibility and processability. For example, the integration of poly(vinylidene fluoride-co-trifluoroethylene) (PVDF-TrFE) with $\text{Li}_6\text{PS}_5\text{Cl}$ [31] has resulted in composite films exhibiting increased conductivities and improved mechanical robustness. Furthermore, advancements in processing techniques, such as electrospinning–infiltration–hot-pressing methods, have enabled the fabrication of thin, flexible composite solid electrolyte membranes composed of argyrodite sulfide $\text{Li}_6\text{PS}_5\text{Cl}$ and PVDF-TrFE. These membranes demonstrate high lithium-ion conductivity and good mechanical ductility, contributing to enhanced cycling performance in SSLBs [32]. In addition to polymer integration, surface modifications have been investigated to improve the moisture stability of sulfide electrolytes. For instance, surface molecular engineering techniques have been employed to enable processing of sulfide solid electrolytes in humid ambient air, thereby extending their applicability in practical battery manufacturing environments [33,34].

3.1.2. Oxide-Based Electrolytes

Oxide-based solid electrolytes, particularly garnet-type $\text{Li}_7\text{La}_3\text{Zr}_2\text{O}_{12}$ (LLZO), are celebrated for their wide electrochemical stability windows, often exceeding 6 V [35]. This broad stability range allows for compatibility with high-voltage cathode materials, expanding the potential energy density of solid-state lithium batteries (SSLBs). LLZO's stability against lithium metal and various cathode materials positions it as a promising candidate for next-generation SSLBs [36]. However, it is important to note that while LLZO exhibits a wide electrochemical window, its stability can be influenced by factors such as the presence of impurities, grain boundaries, and the specific doping elements used. For example, studies have shown that doping LLZO with elements like aluminum (Al), gallium (Ga), or tantalum (Ta) can stabilize its cubic phase at room temperature, which is essential for achieving high ionic conductivity and maintaining electrochemical stability [37].

In terms of mechanical properties, oxide-based electrolytes like LLZO generally exhibit higher hardness and elastic moduli compared to their sulfide counterparts. This mechanical strength contributes to their ability to resist dendrite penetration, a critical factor in enhancing the safety and longevity of SSLBs [38]. For example, LLZO has been reported to have an elastic modulus of approximately 150 GPa and a hardness of around 9 GPa, indicating its robust mechanical nature [39]. However, the inherent brittleness of oxide-based electrolytes can pose challenges during battery assembly and operation, potentially leading to microcracks and increased interfacial resistance. To mitigate these issues, strategies such as doping and the development of composite electrolytes have been employed. Doping LLZO with elements like aluminum or tantalum not only stabilizes its cubic phase but also enhances its sinterability and reduces grain boundary resistance, thereby improving its mechanical and electrochemical performance [37]. Furthermore, incorporating polymers into oxide-based electrolytes can improve flexibility and interfacial contact. For instance, composite electrolytes combining LLZO with polymers like polyethylene oxide (PEO) have been explored to enhance mechanical compliance and reduce interfacial resistance, leading to improved battery performance [40].

3.1.3. Polymer-Based Electrolytes

Polymer-based solid electrolytes (PSEs) represent a distinct class of materials in the development of all-solid-state lithium batteries (SSLBs), offering a unique balance between mechanical adaptability, ease of fabrication, and electrochemical compatibility [41]. Their inherent softness, elasticity, and low-temperature processability stand in stark contrast to the brittle nature of oxide and sulfide-based solid electrolytes, making them particularly suitable for flexible and deformable device architectures. Among the various candidates, polyethylene oxide (PEO) and its derivatives have garnered the most attention due to their excellent lithium salt solvation capabilities and ability to form homogeneous ion-conducting networks when doped with lithium salts such as LiTFSI (lithium bis(trifluoromethanesulfonyl)imide) [42]. The repeating ether oxygen units in PEO coordinate readily with Li^+ ions, creating pathways for ion hopping that are particularly efficient in the amorphous phase [43].

A critical advantage of PSEs lies in their straightforward processability. PEO-based membranes, for instance, can be prepared by solution casting from (common organic solvents, hot-pressing into free-standing films, or by melt-processing methods that are scalable and compatible with roll-to-roll manufacturing) [44]. This is of special relevance in the context of emerging battery formats such as pouch cells, 3D-printed cells, or flexible wearable energy storage devices, where conformability to complex geometries is necessary [43]. Another significant benefit of polymer-based electrolytes is their ability to accommodate large strain without mechanical failure. During lithium plating and stripping, electrode

materials undergo volumetric changes that impose stress at the electrode–electrolyte interface [45]. PSEs can deform elastically and plastically to absorb these stresses, thereby preserving interfacial integrity, reducing delamination risks, and minimizing interfacial resistance buildup over long-term cycling. In contrast, ceramic electrolytes are prone to cracking under similar conditions due to their high elastic moduli and low fracture toughness [9]. The low density of polymers, typically less than $1.0 \text{ g}\cdot\text{cm}^{-3}$, also enables the design of ultralightweight energy storage systems—an attribute that is critical in sectors such as aerospace and biomedical devices where gravimetric energy density is a dominant design criterion. Furthermore, the chemical structure of polymers can be readily tuned by molecular design to incorporate cross-linkable functionalities, ion-conducting moieties, or interpenetrating phases that allow the tailoring of mechanical, thermal, and electrochemical behavior in a way not possible with most inorganic matrices [46].

Despite their many mechanical and processing advantages, polymer electrolytes exhibit one fundamental limitation that restricts their widespread application in high-performance SSLBs: their intrinsically low ionic conductivity at ambient temperature. Most conventional PEO-based electrolytes, when complexed with lithium salts at optimal salt-to-polymer ratios (typically $\text{EO:Li}^+ \approx 8:1$), show room-temperature conductivities in the range of 10^{-7} to $10^{-5} \text{ S}\cdot\text{cm}^{-1}$ [47]. These values fall significantly short of the target conductivity of $\sim 10^{-3} \text{ S}\cdot\text{cm}^{-1}$ required for practical fast-charging and high-power applications. This low conductivity arises primarily from the semi-crystalline nature of PEO. At room temperature, PEO exists predominantly in a crystalline phase, in which the polymer chains are tightly packed and immobilized, impeding the segmental motion necessary for Li^+ transport. Only the amorphous regions contribute effectively to ionic conductivity, and the mobility of lithium ions in these domains is thermally activated. As a result, PEO-based electrolytes tend to exhibit adequate conductivity only at elevated temperatures (e.g., above 60°C), where crystallinity is disrupted and chain dynamics are enhanced [48]. In addition to temperature dependence, the ionic transference number (t^+) of lithium ions in PEO-based electrolytes is often low, typically in the range of 0.2–0.4. This means that a significant portion of the current is carried by the anions, which can lead to concentration gradients during prolonged cycling and exacerbate issues like polarization and interfacial instability. Furthermore, the accumulation of anions near the electrodes can alter the composition of the solid electrolyte interphase (SEI), impacting the long-term stability of the electrolyte-anode interface [49]. Another inherent limitation is related to the dielectric environment provided by the polymer matrix. Although PEO can dissolve lithium salts, its relatively low dielectric constant ($\sim 5\text{--}7$) means that salt dissociation is not complete, particularly at high salt concentrations. This partial dissociation results in the formation of ion pairs and aggregates, which reduce the number of free Li^+ ions available for conduction and lead to non-ideal transport behavior at practical electrolyte thicknesses [50]. Finally, it is worth noting that the electrochemical stability window of conventional polymer electrolytes is generally narrower than that of ceramic-based systems. PEO-based systems are prone to oxidative degradation at voltages above 4.0 V vs. Li/Li^+ , limiting their compatibility with high-voltage cathode materials such as $\text{LiNi}_{0.8}\text{Co}_{0.1}\text{Mn}_{0.1}\text{O}_2$ (NCM811) or LiCoO_2 . This restricts their application range in SSLBs unless special stabilizing additives or interlayers are introduced [51].

3.2. Interface Engineering Techniques

The interface between the lithium metal anode and the solid-state electrolyte (SSE) is a critical focal point in the design of all-solid-state lithium batteries (ASSLBs). Interfacial instability can lead to increased resistance, uneven lithium deposition, and the formation of dendrites, ultimately compromising battery performance and safety. To address these

challenges, several interface engineering strategies have been developed, including surface coatings, artificial interlayers, and electrolyte–electrode modifications [52].

3.2.1. Surface Coatings

In all-solid-state lithium batteries (ASSLBs), the interface between the lithium metal anode and the solid-state electrolyte (SSE) is critical for ensuring battery performance and safety. Surface coatings have emerged as a pivotal strategy to stabilize this interface by forming protective layers that mitigate undesirable reactions, suppress dendrite formation, and enhance mechanical integrity [53]. One of the primary functions of surface coatings is to enhance the chemical stability at the Li/SSE interface. Materials such as lithium phosphorus oxynitride (LiPON) have demonstrated exceptional stability when interfaced with lithium metal. LiPON forms a stable solid electrolyte interphase (SEI) that effectively suppresses side reactions and reduces interfacial resistance. Studies utilizing cryogenic electron microscopy have revealed that the Li/LiPON interface exhibits a multilayer mosaic SEI structure with concentration gradients of nitrogen and phosphorus, contributing to its stability and resistance to dendrite formation [54]. Furthermore, the application of LiPON coatings on SSEs has been shown to improve the long-term stability against lithium, making it a promising candidate for enhancing the chemical compatibility at the interface [55]. Surface coatings also serve as mechanical barriers that reinforce the interface, suppressing dendrite penetration and accommodating volume changes during cycling. Aluminum oxide (Al_2O_3), applied via atomic layer deposition (ALD), is a notable example. ALD allows for the deposition of uniform and conformal Al_2O_3 layers with precise thickness control, enabling the formation of robust interfacial layers that can withstand the mechanical stresses during lithium plating and stripping. These coatings not only enhance the mechanical strength but also contribute to the suppression of lithium dendrite growth. First-principles studies have further elucidated the role of amorphous Al_2O_3 coatings, applied via atomic layer deposition (ALD), in lithium–sulfur battery electrodes, demonstrating their effectiveness in mitigating the shuttle effect of soluble polysulfides and enhancing the mechanical stability of the electrode [56]. Surface coatings contribute significantly to the electrochemical performance of ASSLBs by facilitating uniform lithium-ion flux and reducing the formation of high-resistance interphases. For example, the application of ultrathin Al_2O_3 layers via ALD on SSE surfaces has been demonstrated to effectively suppress lithium dendrite growth and enhance the cycling stability of ASSLBs. These coatings act as artificial SEI layers that provide a stable and conductive pathway for lithium ions while preventing electronic conduction that could lead to dendrite formation [57]. Additionally, the integration of surface coatings such as LiPON and Al_2O_3 has been shown to improve the interfacial adhesion and reduce the interfacial resistance between the SSE and the lithium metal anode, thereby enhancing the overall electrochemical performance of the battery.

3.2.2. Artificial Interlayers

In all-solid-state lithium batteries (ASSLBs), the interface between the lithium metal anode and the solid-state electrolyte (SSE) is critical for ensuring battery performance and safety. Artificial interlayers have emerged as a pivotal strategy to promote uniform lithium deposition, suppress dendrite formation, and enhance interfacial stability. These engineered materials are inserted between the lithium anode and the SSE and can be designed to possess specific properties:

- (i). Lithiophilic materials serve to reduce the energy barrier for lithium nucleation and guide uniform lithium deposition. Metals such as silver (Ag), zinc (Zn), and tin (Sn), or their alloys, are widely employed due to their favorable interactions with lithium. For example, Zhang et al. reported a layer-by-layer lithiophilic-electron-blocking interfacial design consisting of Sn, LiF, and Li₂CO₃, which effectively guided lithium nucleation while suppressing electron leakage and parasitic reactions, enabling long-term cycling in Li/SSE cells even at elevated temperatures [58]. Pang et al. explored an alternative strategy by introducing silver nanoparticles at the interface between Li₆PS₅Cl and metallic lithium, enabling a detailed study of interfacial behavior [59]. The Ag nanoparticles promote the suppression of lithium dendrites via the formation of Li–Ag alloy phases [59].
- (ii). Ion Conductivity: Effective interlayers must also facilitate fast and homogeneous lithium-ion transport. To this end, ion-conductive ceramics (e.g., Li₃N, Li_{1.5}Al_{0.5}Ge_{1.5}(PO₄)₃, or Li₇La₃Zr₂O₁₂ nanoparticles) and solid polymer electrolytes (e.g., PEO-LiTFSI, Li-rich SEI layers) have been employed as interlayers. For instance, Wan et al. developed a composite interlayer composed of a Li₃N–polymer hybrid that exhibited high ionic conductivity ($\sim 10^{-3}$ S·cm⁻¹) and formed a stable Li₃N-based SEI during cycling, significantly enhancing Li/SSE interfacial compatibility [60]. Similarly, Hoang et al. developed a low-cost method to spontaneously form protective polymer layers on lithium metal using acrylonitrile, extending the anode's lifetime sixfold under high current cycling [61]. The treated Li anodes showed improved interfacial stability and reduced overpotential when paired with LGPS solid-state electrolytes [61].
- (iii). Mechanical Compliance: Flexible interlayers can accommodate volume changes during cycling, maintaining intimate contact between the anode and SSE. In situ construction of a flexible interlayer has been reported to enhance the durability of solid-state lithium metal batteries [62].
- (iv). Multifunctional Composite Interlayers: The most effective interlayers often combine multiple features. A representative example is the dual-component LiSn–Li₃N interlayer reported by Ren et al., which forms in situ at the Li/SSE interface [63]. The LiSn alloy promotes uniform lithium deposition via its high lithium diffusivity, while the Li₃N component contributes both ionic conductivity and mechanical reinforcement. This multifunctional interface not only blocked dendrite propagation but also reduced interfacial resistance and enhanced battery stability over extended cycles [63,64]. Another example is the use of a TiO₂–polyimide nanofiber interfacial layer, which provides ionic pathways, mechanical flexibility, and lithiophilicity simultaneously, reducing the onset voltage of lithium nucleation and eliminating voids that lead to dendrite growth [65].

3.2.3. Electrolyte–Electrode Modifications

In all-solid-state lithium batteries (ASSLBs), the interface between the solid-state electrolyte (SSE) and the electrodes plays a pivotal role in determining the overall performance and safety of the battery. Modifying this interface is crucial for enhancing stability, reducing interfacial resistance, and preventing the formation of lithium dendrites [66]. Several strategies have been developed to address these challenges, including the use of chemical additives, structural engineering, and interface passivation techniques. Incorporating specific chemical additives into the electrolyte can significantly improve the stability of the solid electrolyte interphase (SEI) [67]. For example, fluoroethylene carbonate (FEC) has been widely studied for its ability to form a stable and robust SEI layer. The presence of FEC in the electrolyte leads to the formation of a thinner and more elastic SEI, which

enhances the electrochemical performance and cycling stability of the battery. Studies have shown that FEC-modified electrolytes result in improved interfacial stability and reduced impedance growth during cycling [68].

Designing the microstructure of the electrode to have a porous or three-dimensional (3D) architecture can facilitate better contact with the SSE and accommodate volume changes during cycling. Such architectures increase the effective contact area between the electrode and the electrolyte, leading to enhanced ion transport and reduced interfacial resistance. For example, the use of 3D porous copper composites as anodes has been shown to provide robust frameworks that support uniform lithium deposition and mitigate dendrite formation [69]. Applying passivation layers or coatings on the electrode surface can prevent undesirable reactions with the SSE, enhancing interfacial compatibility. These passivation layers act as protective barriers that suppress side reactions and stabilize the interface. For instance, the formation of a solid electrolyte interphase (SEI) through the decomposition of electrolyte additives like FEC can effectively passivate the electrode surface, leading to improved cycling performance and longevity.

Localized dendrite growth is a significant concern in ASSLBs, as it can lead to short circuits and battery failure. To prevent this, several approaches have been explored:

(i). Electron-Blocking Interlayers

Introducing interlayers that are ionically conductive but electronically insulating can prevent electron leakage, which is a precursor to dendrite formation. For example, a study demonstrated that a lithophilic and electron-blocking multilayer interlayer substantially enhanced the performance of lithium metal batteries by suppressing dendrite growth and improving interfacial stability [58]. In another recent work, Li₃N-based interlayers deposited between Li and garnet SSEs acted as fast-ion conductors while blocking electron tunneling, resulting in lower interfacial impedance and extended cycling life [63].

(ii). Mechanical Reinforcement

Enhancing the mechanical strength of the SSE or incorporating reinforcing agents can resist dendrite penetration. Materials with higher mechanical moduli can better withstand the stresses induced during lithium plating and stripping, thereby suppressing dendrite propagation. For instance, the use of amorphous Li-La-Zr-O coatings has been shown to act as effective dendrite-blocking layers due to their grain-boundary-free microstructure and high electronic insulation [70].

(iii). Uniform Current Distribution

Ensuring a uniform current distribution across the electrode surface can minimize hotspots that lead to dendrite initiation. Strategies such as designing electrodes with uniform pore sizes and incorporating materials that facilitate homogeneous lithium-ion flux can contribute to uniform current distribution. For example, Zhang et al. demonstrated that a gradient Li₃BO₃ gradient coating effectively distributed the current density and suppressed dendritic protrusions by creating a favorable lithium-ion conduction gradient and increasing the cell capacity [71]. In another study, the construction of a three-dimensional continuous Li⁺-conducting and electron-blocking grain boundary network based on Li_{1.3}Al_{0.3}Ti_{1.7}(PO₄)₃ enhanced ion transport while preventing electronic shorting, leading to stable cycling at high current densities [72].

3.3. Mechanical Design Approaches for Dendrite Suppression

In addition to chemical and interfacial modifications, mechanical design strategies are increasingly recognized as effective means to mitigate lithium dendrite formation in solid-state lithium batteries (SSLBs). These approaches aim not only to increase the intrinsic mechanical strength of the solid electrolyte but also to regulate lithium growth by

tailoring the physical architecture of the electrode–electrolyte system. Fundamentally, the nucleation and propagation of dendrites are mechanically driven phenomena, sensitive to local stresses, modulus mismatch, and volumetric fluctuations during lithium plating and stripping. Therefore, reinforcing the electrolyte matrix, accommodating dynamic deformations, and guiding lithium morphology through geometrical constraints can significantly delay or suppress dendrite intrusion. Recent research has explored several directions under the umbrella of mechanical design, including (i) nanocomposite electrolytes incorporating high-modulus fillers to enhance toughness and ion transport, (ii) self-healing materials that can dynamically repair internal cracks or voids generated during cycling, (iii) gradient or multilayered electrolytes with spatially tailored properties that balance rigidity and interfacial contact, and (iv) three-dimensional (3D) structured electrodes and current collectors designed to modulate the current distribution and confine lithium within architected porous hosts. Each of these strategies introduces specific mechanical constraints or adaptive responses that reshape lithium behavior at the mesoscale, ultimately enabling more uniform and reversible lithium deposition. In the following subsections, we examine these mechanical design approaches in detail, discussing their implementation, underlying mechanisms, and recent advancements supported by experimental evidence [73].

3.3.1. Nanomaterials and Composite Structures for Reinforcement and Ion Transport

Incorporating nanomaterials into solid-state electrolytes has emerged as an effective strategy to improve mechanical strength without sacrificing ionic conductivity. Rigid ceramic fillers (e.g., $\text{Li}_7\text{La}_3\text{Zr}_2\text{O}_{12}$, Al_2O_3) dispersed in polymer electrolytes can increase the elastic modulus and toughness of the electrolyte while also creating additional Li^+ conduction pathways [74,75]. For example, adding graphene-based materials to polymer electrolytes has been shown to both reinforce the mechanical matrix and reduce polymer crystallinity, thereby enhancing Li^+ conductivity [74]. Zhang et al. functionalized graphene oxide (GO) with poly(ionic liquid) chains to achieve a uniform GO dispersion in a PEO electrolyte, which lowered crystallinity and enabled a $\text{Li} \parallel \text{Li}$ cell to cycle much longer without short-circuiting compared to an unfilled PEO electrolyte [76]. Aligning 2D nanofillers within polymer matrices can enhance performance by guiding ion transport along the oriented sheets, resulting in anisotropically high ionic conductivity [74,76,77]. These graphene-based composite electrolytes exhibit higher critical current densities for dendrite-free operation by virtue of their increased stiffness and more homogeneous ion transport network.

Nanomaterials have also been used to reinforce brittle inorganic solid electrolytes. While ceramic electrolytes are intrinsically stiff, their low fracture toughness means that tiny cracks can act as conduits for dendrites [74,78]. Adding a minor fraction of reduced graphene oxide (rGO) platelets to a ceramic Li-Al-Ti-P oxide (LATP) electrolyte was found to double its fracture toughness from ~ 1.1 to $2.4 \text{ MPa}\cdot\text{m}^{0.5}$ by a crack-bridging mechanism [74,78]. The rGO-reinforced LATP showed no signs of dendritic short-circuit in $\text{Li} // \text{Li}$ symmetric cells over >250 h, whereas the pristine LATP would typically succumb to fracture-assisted Li infiltration [74]. Graphene's extraordinary mechanical strength (Young's modulus ~ 1 TPa) allows it to act as a "nano-rebar," deflecting and blunting cracks that would otherwise enable dendrite propagation [79,80]. Importantly, an optimized low loading (~ 1 vol% rGO) is used to avoid percolating electronic pathways [74], thus maintaining a high ionic/electronic selectivity. Beyond carbon, 2D inorganic additives like molybdenum disulfide (MoS_2) have been employed as protective interlayers to stabilize the Li interface. MoS_2 coatings on garnet-type electrolytes (e.g., LLZO) form a lithiated conversion layer ($\text{Li}_2\text{S}/\text{Mo}$) that is ion-conductive but electronically insulating, effectively blocking electron-fed dendrite growth [81]. In one study, a thin MoS_2 interlayer on LLZO

dramatically flattened the Li stripping/plating voltage profile and prevented dendrites from penetrating along grain boundaries [82]. The lithophilic MoS₂ layer improved interfacial wetting and then transformed into a robust solid-electrolyte interphase that suppressed local dendrite nucleation, enforcing a more uniform Li deposition [82]. Overall, composite design using nanomaterials (graphene, MoS₂, etc.) imbues the electrolyte with high mechanical resilience and controlled ion pathways, raising the dendrite initiation barrier and promoting more even lithium distribution across the interface.

3.3.2. Self-Healing Materials and Adaptive Interfaces

A cutting-edge approach to dendrite suppression is the development of self-healing solid electrolytes that can autonomously repair the microscopic damage associated with dendrite growth. During cycling, stress and lithium plating can induce nano-cracks, voids, or other defects in the electrolyte; these defects concentrate current and become hot-spots for dendrite initiation [83]. Self-healing electrolytes address this by incorporating dynamic chemical bonds or flowable components that allow the material to recover its integrity after damage. For example, recent studies have designed polymers with reversible crosslinks (such as hydrogen bonds, imine bonds, or disulfide bonds) that break and reform, enabling the polymer to mend cracks caused by lithium filament pressure [84,85]. The rational design of such self-healing polymer networks is intended to inhibit crack propagation and maintain intimate contact at the Li/electrolyte interface during cycling [86]. He et al. reported a “plastic crystal” composite electrolyte using a dynamically crosslinked polymer (with non-covalent $-\text{CH}_3 \dots \text{CF}_3$ interactions) integrated with a ceramic filler [83]. This electrolyte exhibited a two-step self-healing mechanism where micro-cracks were first filled by the mobile polymer matrix and then fully repaired via polymer re-crosslinking [83]. Remarkably, the self-healing composite suppressed the formation of any high-current dendrite pathways (“hotspots”) and sustained dendrite-free cycling for over 2000 h at 1 mA cm⁻² in Li | Li tests [83]. Post-mortem analysis confirmed that internal defects which would normally lead to filament growth were eliminated by the self-healing process [83]. Besides extending cell lifetime, this approach improves lithium deposition uniformity by constantly smoothing out the Li/electrolyte interface. Operando X-ray fluorescence (XRF) microscopy has recently enabled direct visualization of this healing mechanism. Figure 1 illustrates the dynamic closure of voids during electrochemical cycling, confirming that the plastic ceramic electrolyte not only adapts to mechanical stress but actively repairs damage at the microscale. The experiment reveals polymer infiltration followed by ceramic migration, validating the two-step healing process under real battery conditions. Other reports of self-healing polymer electrolytes (using, e.g., urethane–urea hydrogen bonding or disulfide linkers) similarly show that dendrite-induced cracks/voids can be spontaneously repaired, thereby preventing isolated “dead lithium” pockets and maintaining even lithium plating [87]. While still an emerging technology, self-healing solid electrolytes offer a dynamic means of arresting dendrite growth *in situ*, effectively combining mechanical resilience with adaptivity to achieve long-term dendrite suppression.

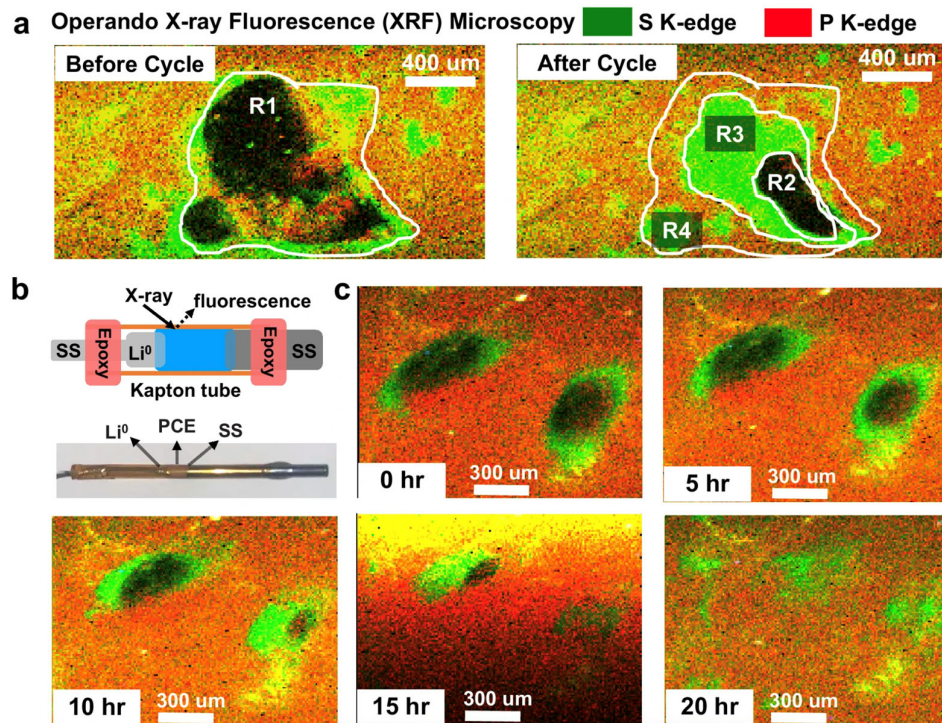


Figure 1. Self-healing behavior of plastic ceramic electrolyte (PCE) revealed by operando X-ray fluorescence (XRF) microscopy. (a) Elemental mapping images of sulfur (green) and phosphorus (red) before and after electrochemical cycling show polymer and ceramic components migrating into a pre-existing void at the Li/SSE interface. The color changes indicate redistribution of the dual-phase system during the healing process. (b) Schematic representation of the in situ XRF setup using a customized Kapton tube cell for simultaneous electrochemical operation and spatially resolved elemental analysis. This configuration enables non-invasive visualization of internal dynamics in real time. (c) Time-resolved XRF elemental maps over a 20 h cycling period demonstrate progressive void closure driven by cooperative infiltration of polymer and ceramic phases. Initially empty interfacial defects are gradually filled, validating the two-step self-healing mechanism. (Adapted with permission from ref. [83], Springer Nature 2024).

3.3.3. Gradient and Multilayer Electrolytes

Functionally graded electrolytes have been introduced as an innovative design to combine the best attributes of different materials and mitigate dendrites. Instead of a uniform single-phase electrolyte, a gradient structure gradually varies the composition or mechanical properties across the thickness. The rationale is to use a stiffer, dendrite-resistant layer at the lithium interface and a more compliant, interface-friendly layer toward the cathode, avoiding abrupt interfaces that can cause stress or impedance. A recent example is a gradient composite solid electrolyte (GCSE) in which a ceramic filler content transitions from high in the central region to lower at the outer faces [88]. Zhang et al. (2024) implemented this by dispersing $\text{Li}_{6.4}\text{La}_3\text{Zr}_{1.4}\text{Ta}_{0.6}\text{O}_{12}$ (LLZTO) particles in a polymer matrix with a controlled spatial gradient: the core of the membrane is rich in LLZTO (imparting high hardness to block dendrites), while the surfaces are richer in pliable polymer (enhancing contact with electrodes) [88]. This smoothly graded architecture provided multiple benefits—the ceramic-rich center acted as a strong barrier against lithium penetration, and the polymer-rich sides improved interfacial compatibility and reduced contact resistance [88]. Crucially, the continuous gradient avoided any sharp interfaces between hard and soft layers, facilitating uniform Li^+ flux and minimizing internal stress concentrations. The GCSE achieved a high room-temperature ionic conductivity ($\sim 1.5 \times 10^{-4} \text{ S}\cdot\text{cm}^{-1}$) and enabled stable lithium plating for over 1200 h in symmetric cells with no short-circuit [88]. In full cells ($\text{Li} \parallel \text{LFP}$),

the graded electrolyte delivered improved cycling stability and capacity retention relative to a homogeneous composite [88]. Similar multi-layer or functionally graded designs have been reported by other groups—for example, bilayer electrolytes where an ultrathin, high-modulus inorganic layer is laminated onto a flexible organic layer to simultaneously resist dendrites and lower interfacial impedance [89,90]. Such gradient electrolytes leverage spatial material distribution as a design knob to localize the strongest mechanical protection exactly where needed (near the Li anode) while still ensuring fast ion transport and good electrode integration. By tailoring the electrolyte’s internal architecture, researchers are effectively spreading out the lithium deposition uniformly and preventing the formation of concentrated dendritic channels.

3.3.4. 3D-Structured Anodes and Current Collectors

In addition to engineering the electrolyte, three-dimensional structured electrodes provide a mechanical means to regulate lithium growth. The concept is to host lithium within a conductive porous scaffold or framework, rather than depositing onto a flat surface, thereby reducing local current densities and accommodating volume changes. Extensive work on 3D Li metal hosts has shown that increasing the effective surface area for Li plating leads to smoother, dendrite-free deposition [91–93]. Porous metal foams, woven meshes, carbon networks, and 3D-printed frameworks have all been explored as scaffolds that lithium can infuse into. These conductive 3D hosts draw plating into their interior void space (rather than protruding outward), which both lowers the propensity for needle-like dendrites and buffers the large 100% volume expansion of Li metal [92]. For instance, Hu’s group demonstrated that a carbon nanotube sponge with an alumina-coated surface provides a high-surface-area network where Li can nucleate on many sites; as a result, dendrite growth was effectively suppressed and Coulombic efficiency doubled compared to a planar Li foil anode [94]. The mechanical stability of the scaffold and the presence of lithiophilic surfaces (e.g., ALD-Al₂O₃ or other seed layers) are key to achieving uniform Li distribution. Xu et al. reported a graphene/MgF₂ hybrid framework that, after molten lithium infusion, formed a robust 3D Li-metal anode [95]. The rigid rGO network maintained structural integrity during cycling while nanoscale MgF₂ lithiophilic sites ensured even nucleation of Li—yielding stable stripping/plating for ~450 h at 1 mA cm⁻² with no dendrite failure [95]. The structural features and compositional distribution of this composite are shown in Figure 2.

Advanced 3D host designs increasingly focus on graded porosity and surface modifications to further homogenize the lithium deposition. Lee et al. [96] showed that a gradient pore size copper scaffold (with pores getting smaller with depth) induces “superconformal” lithium growth throughout the 3D matrix, as opposed to Li accumulating only near the entrance of uniform pores. The gradient-pore Cu host achieved 760 cycles at 2 mA cm⁻² with no short-circuit, outliving a comparable scaffold with monodisperse pores by virtue of its more uniform Li distribution in 3D [96]. In another approach, an electrospun copper nanofiber (Cu-CNF) scaffold was decorated with ultrafine Cu particles to nucleate lithium evenly across the framework [97]. The lithiophilic Cu seeds promoted uniform initial lithium plating, while the 3D CNF network guided the continued growth within its conductive filaments. This Cu-CNF host enabled remarkable cycling stability—a Li||Li cell endured 500 h at 5 mA cm⁻² without dendritic shorting, whereas a control carbon scaffold without the Cu seeds showed erratic plating and premature failure [97]. These examples illustrate how 3D structured anodes effectively disperse the electrochemical deposition of lithium over a large area/volume, preventing any single point from developing a dendritic protrusion. Moreover, by confining lithium in a scaffold, the plated metal forms a smooth filling of the porous matrix rather than extending outward as needles [98]. The result is

a more uniform lithium morphology and improved safety and reversibility of Li-metal anodes. Going forward, combining 3D hosts with solid-state electrolytes (for example, a lithium-infused porous framework integrated with a stiff separator) is a compelling direction to synergistically use mechanical design for dendrite suppression [93,99]. In summary, 3D structured electrodes exemplify mechanical ingenuity—using architectural design to tame lithium dendrites by giving lithium pre-defined, dendrite-averse spaces in which to deposit.

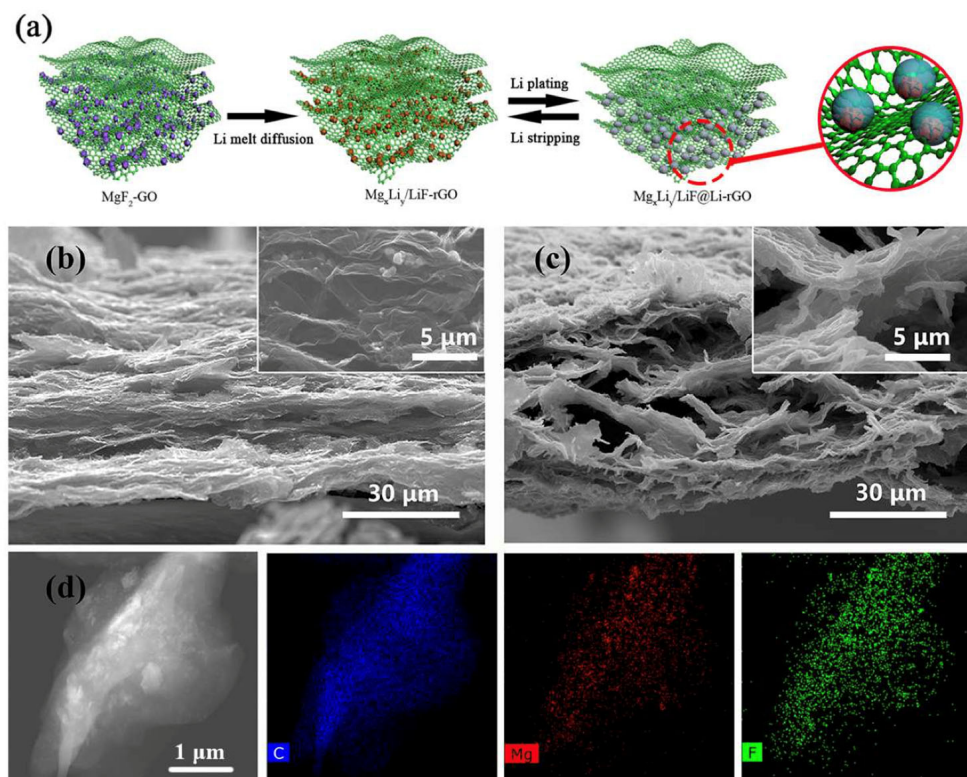


Figure 2. (a) Schematic diagram illustrating the fabrication process and function of the composite architecture. Molten lithium infiltrates a porous rGO framework pre-coated with MgF_2 nanoparticles, creating a hybrid scaffold with chemically and mechanically engineered lithiophilicity. The resulting anode supports uniform lithium plating and stripping within the 3D matrix. (b) Cross-sectional SEM image of the MgF_2 -rGO scaffold before lithium infusion, showing the highly porous and interconnected microstructure intended to host lithium uniformly. (c) SEM image of the same region after lithium melt infiltration, where the voids are filled with metallic lithium, confirming successful infusion into the scaffold. The structure retains mechanical integrity and enables expansion accommodation. (d) High-angle annular dark-field (HAADF) STEM image of the composite, combined with energy-dispersive X-ray (EDX) elemental mapping, confirms homogeneous distribution of carbon (C), magnesium (Mg), and fluorine (F) throughout the scaffold, indicating effective dispersion of MgF_2 within the rGO matrix. (Adapted with permission from ref. [95], Elsevier 2020).

To synthesize the different strategies examined in previous sections Table 1 provides a comparative overview of recent dendrite suppression approaches. It highlights their respective advantages, technical challenges, and representative studies, serving as a practical reference for researchers developing next-generation SSLBs.

Table 1. Comparative overview of recent dendrite suppression strategies and potential limitations in solid-state lithium batteries.

Strategy	Main Advantage	Key Challenge	Main Limitation	Reference
Interface Coatings	Enhances chemical stability at the Li/SSE interface	Maintaining ionic conductivity across coating layer	Coatings may delaminate or crack during cycling; non-uniform layers may create local resistances	[57]
Electron-Blocking Interlayers	Suppresses electron flow, blocks dendrite growth	Complex fabrication and interface compatibility	Added layers can increase interfacial resistance; limited thermal/mechanical stability under extended cycling	[58]
Polymer–Ceramic Composite Electrolytes	Combines mechanical flexibility and ionic conductivity	Achieving uniform dispersion and phase stability	Inhomogeneous ceramic distribution may cause local stress or poor Li ⁺ transport; processing complexity	[100]
Doping of SSEs	Improves ionic conductivity and structural robustness	Controlling dopant homogeneity and effects	Excessive or poorly distributed dopants can destabilize phase purity or reduce mechanical strength	[101]
3D-Host Architectures	Reduces local current density, directs Li deposition	Fabrication scalability and maintaining conductivity	May reduce volumetric energy density; mechanical degradation or clogging of pores over long-term cycling	[102]
LiH Mitigation	Avoids formation of electronically insulating LiH phases	Complete elimination of hydrogen sources is difficult	Residual moisture or parasitic reactions may still generate LiH; suppression is not fully effective in ambient setups	[103]

3.4. Advanced Characterization Techniques

Advanced characterization methods have become indispensable for understanding and mitigating lithium dendrite formation in solid-state batteries. In situ/operando electron microscopy and various spectroscopic techniques allow researchers to directly observe dendrite behavior, probe interfacial chemistry, and evaluate the effectiveness of dendrite suppression strategies in real time. These tools provide complementary insights: electron microscopy visualizes the nucleation and propagation of Li filaments under realistic conditions, while spectroscopy reveals chemical, electrochemical, and even mechanical aspects of interfaces that govern dendrite growth or suppression. Below, we review recent advances (2022–2025) in applying these techniques to solid-state lithium batteries, highlighting how they have been used to observe dendrite formation, quantify its effects, and guide the design of interface engineering and material innovations for dendrite suppression.

In situ electron microscopy (including transmission electron microscopy, TEM, and scanning electron microscopy, SEM) enables real-time monitoring of dendrite formation and propagation at nanometer to atomic scales. Recent studies have leveraged specialized operando TEM cells and environmental SEM setups to visualize how Li dendrites initiate and penetrate solid electrolytes during battery operation [104]. These experiments provide direct evidence of electro-chemo-mechanical processes at the Li/SSE interface that were previously inferred only indirectly. For example, Gao et al. used in situ TEM to observe Li plating against a garnet-type electrolyte (LLZO) under controlled pressure and current conditions [105]. They constructed a Cu|LLZO|Li nanobattery and directly visualized how Li deposition-induced stress, depending on the mechanical constraint and local current density, leads to various interfacial behaviors. At low current density and under strong uniaxial pressure, Li expanded laterally via creep, preserving the LLZO integrity. However, under rapid deposition (“Li eruption”), they observed the sudden nucleation of cracks—even in pristine single-crystal LLZO particles—driven by stress accumulation surpassing $3 \text{ A}\cdot\text{cm}^{-2}$ and generating GPa-level pressures. This dynamic visualization demonstrated that dendrite-induced stress can fracture a stiff ceramic electrolyte, and it revealed that the mode of Li growth (lateral vs. vertical extrusion) strongly influences

whether the solid electrolyte cracks or remains intact [105]. Figure 3 summarizes these contrasting growth modes: while slow, pressure-modulated extrusion enables stable lateral expansion, fast vertical eruption leads to mechanical failure. Such results underscore that not only current density but also stress release pathways at the interface dictate dendrite penetration, knowledge that is guiding strategies to accommodate or redirect stress in solid-state cells. Operando electron microscopy has also been used to compare dendrite behavior with and without interface modifications. A notable 2025 study by Zhao et al. employed an operando SEM to monitor the Li–electrolyte interface in a sulfide-based solid battery under realistic conditions [104]. By imaging the cross-section of a Li metal anode stripping from $\text{Li}_6\text{PS}_5\text{Cl}$ (LPSCl) electrolyte, they visualized how voids form and evolve at the interface. Pure Li anodes developed multiple small voids during stripping that eventually coalesced into a large crack, leading to interfacial delamination [104]. In contrast, an alloyed Li–Mg anode showed a very different behavior: the initial voids were more numerous but tended to split and collapse, which partially preserved contact between the metal and SSE [104]. This real-time observation explained the improved performance of Li–Mg alloy anodes, the Mg incorporation changes interfacial dynamics so that voids do not unite into a continuous gap. Density functional theory (DFT) calculations confirmed that Mg has a strong affinity for the sulfur in the SSE, which draws Mg toward the interface and prevents lithium void accumulation by pushing Li vacancies into the bulk metal [104]. The SEM study directly correlating void dynamics with electrochemical behavior illustrated an important suppression mechanism: alloying the Li anode can maintain interfacial contact and delay the onset of dendritic short-circuit by reducing void-induced hotspots [104]. Beyond standard TEM/SEM, researchers have developed creative adaptations to visualize Li dendrites under more battery-like conditions. For instance, cryo-electron microscopy (cryo-EM) has been used to examine dendrites and interphases post-mortem by freezing battery samples to preserve delicate Li filaments. Using cryo-TEM, Vilá et al. and others revealed that lithium dendrites often contain lithium hydride (LiH) as a major component [103]. This LiH, which forms due to side reactions with trace amounts of moisture or electrolyte components, is electronically insulating. It traps active lithium within the dendrite structure, rendering it electrochemically inactive and thereby accelerating capacity loss [103]. Identification of LiH in dendrites (observed in both liquid and solid electrolytes) highlights the critical role of interfacial chemistry in dendritic failure and suggests that eliminating hydrogen sources or preventing LiH formation could be a strategic route to mitigate dendrite-related losses. Recent cryo-electron microscopy and spectroscopy studies confirm that LiH forms as a by-product of electrolyte decomposition at the lithium interface, and its accumulation can electrically isolate active lithium, reducing battery capacity. In another approach combining microscopy and mechanical analysis, advanced setups have paired TEM with atomic force microscopy. For example, Zhang et al. [106] employed an *in situ* AFM–ETEM system to measure the stress generated by growing “lithium whiskers” (filamentary Li). They found that these whiskers can exert stresses up to 130 MPa, which is sufficient to deflect or blunt dendritic growth [106]. Although this study predates 2022, its methodology continues to inspire recent work linking real-time microscopy observations with mechanical forces in dendritic evolution.

Indeed, Yildirim et al. recently used operando X-ray microscopy alongside optical imaging to show that Li dendrites growing in single-crystal LLZTO induce dislocations in the crystal lattice near the dendrite tip [20]. These stress-induced lattice defects can in turn guide the dendrite’s path and branching behavior [20]. Such multi-modal microscopy studies provide a holistic picture of dendrite propagation, wherein one can see the interplay of electrochemical deposition, mechanical stress, and microstructure of the solid electrolyte in real time. *In situ* electron microscopy techniques have thus allowed direct observation

of dendrite nucleation sites, growth kinetics, and the effect of interventions (pressure, alloying, coatings, etc.) on dendrite suppression. The ability to watch a dendrite penetrate or be stopped by a modified interface is incredibly valuable for verifying suppression mechanisms. These techniques, however, must contend with challenges like the reactivity of Li in vacuum and the need for specialized cells or low-dose imaging to avoid beam damage. Despite these challenges, rapid progress is being made. For example, modern TEM holders now allow biasing and even heating of solid-state cell specimens, effectively creating “micro-batteries” inside the microscope [105]. In summary, operando electron microscopy has emerged as a powerful tool to directly witness dendrite formation and its prevention, yielding insights into failure mechanisms (e.g., stress-induced cracking, grain boundary transport pathways) that inform the design of more robust solid-state interfaces.

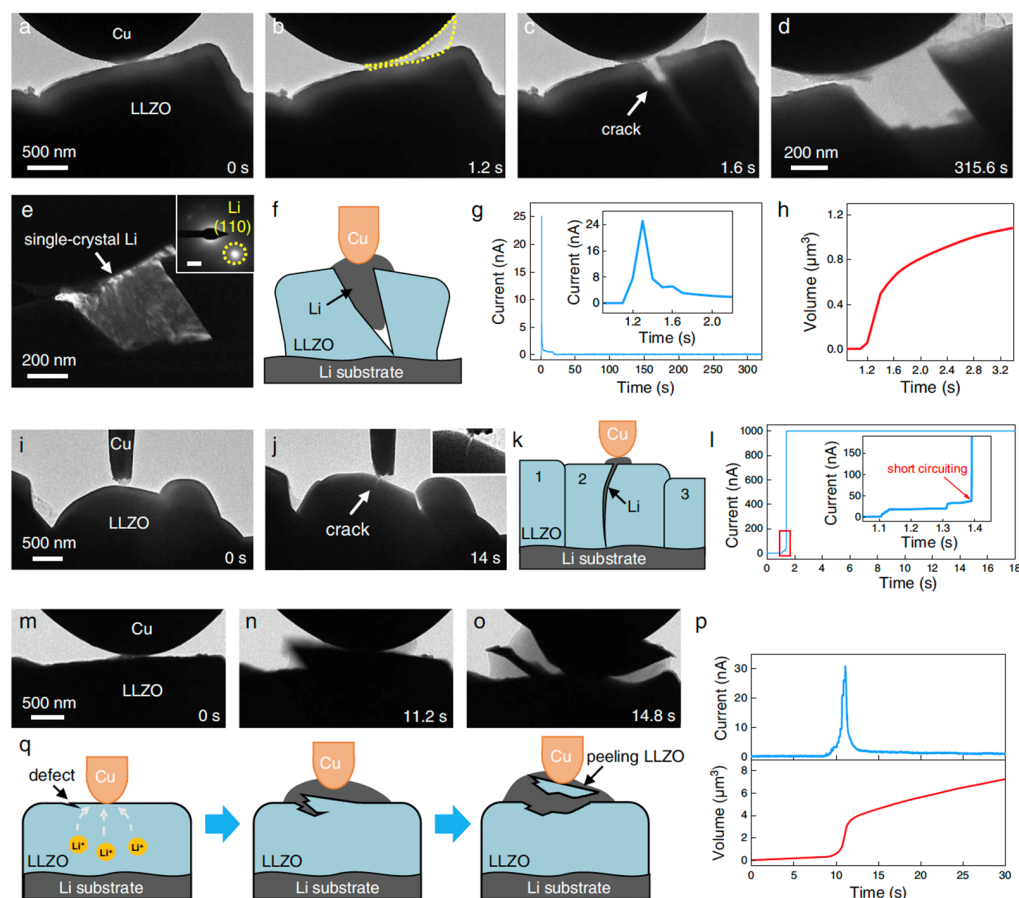


Figure 3. Operando visualization of fracture and lithium dendrite penetration in single-crystal LLZO under varying interfacial stress conditions. (a–c) Sequential imaging of lithium metal deposition against a constrained Cu | LLZO interface, showing Li eruption and stress accumulation that eventually lead to fracture in the solid electrolyte. (d–f) After fracture, lithium infiltrates the crack and propagates into the bulk LLZO, ultimately splitting the entire crystal particle. (g,h) Electrochemical and volumetric data (current and volume traces) recorded simultaneously with imaging reveal the onset of mechanical failure, correlating abrupt volume changes with interfacial breakdown. (i–k) Under mechanical confinement, lithium plating proceeds via lateral extrusion (instead of vertical eruption), enabling mechanically stable growth without cracking. (l–n) Comparative imaging of the two growth modes (rupture vs. extrusion) illustrates the critical role of stress modulation in determining dendrite path. (o–q) Schematic representations summarize the mechanisms: without pressure, rapid Li deposition leads to vertical stress accumulation and rupture; under applied pressure, Li grows laterally via plastic deformation of the interface. (Adapted with permission from ref. [105], Springer Nature 2022).

While imaging reveals where and how dendrites grow, spectroscopy techniques probe the chemical and physical state of materials before, during, and after dendrite formation. They are essential for analyzing the electrochemical and mechanical properties of interfaces and for evaluating dendrite suppression mechanisms at a molecular level. Key spectroscopic methods include surface analytical techniques (X-ray photoelectron spectroscopy and secondary-ion mass spectrometry), vibrational spectroscopies (Raman), nuclear magnetic resonance, and impedance spectroscopy. Each offers unique information that complements microscopy, helping to build a complete picture of dendrite behavior in solid-state batteries. X-ray Photoelectron Spectroscopy (XPS) is widely used to analyze surface chemistry at the Li anode–electrolyte interface. In solid-state cells, XPS can identify the compositions and oxidation states of elements in the solid-electrolyte interphase (SEI) or interfacial layers that form during cycling. Recent studies have employed *in situ* XPS to monitor these interphase changes as lithium is plated/stripped. For example, Zaccarine et al. designed a thin polymer/thiophosphate composite electrolyte and used *in situ* XPS (with a built-in Li deposition apparatus) to observe the formation of a LiF-rich SEI at the interface during the first minutes of lithium plating [107]. The XPS spectra showed that as Li metal was deposited onto the composite SSE, species from the Li salt (LiFSI) decomposed to form LiF and lithium sulfide (Li_2S) species, while harmful components like $-\text{SO}_2\text{F}$ groups were consumed [108]. This LiF-rich interphase correlated with a more stable interface: concomitant electrochemical testing showed that cells with the modified SSE had lower interfacial impedance growth and suppressed dendrite formation [107]. In other words, XPS directly verified that the polymer-sulfide composite created a stable, dendrite-suppressing SEI rich in LiF (a known electronic insulator and ion-conductor), which protected the Li metal. XPS has also been applied *ex situ* to failed cells to identify fingerprints of dendritic failure—for instance, detecting reduced sulfur species or elemental Li within the SSE, which indicate lithium penetration. Because XPS is surface-sensitive (probing a few nanometers deep), it is especially useful for examining interfacial layers that may dictate whether a dendrite can initiate. Modern synchrotron XPS with nano-focusing has even been performed *operando*, providing spatially resolved chemical information at interfaces. Overall, XPS helps answer what chemical species are present at the interface and how interface chemistry evolves when a certain suppression strategy (e.g., additives, coatings) is used. Time-of-Flight Secondary Ion Mass Spectrometry (ToF-SIMS) complements XPS by mapping the spatial distribution of elements (particularly Li) and molecules in three dimensions. In solid-state batteries, ToF-SIMS depth profiling can reveal whether lithium has penetrated along grain boundaries or cracks in the electrolyte. For example, ToF-SIMS was used to examine LLZO garnet after cycling and found lithium enrichment along certain grain boundaries, correlating with observed filament paths [109]. In a recent study of solid-state cell failure, ToF-SIMS provided “plane view” maps of interfacial degradation: regions of the Li anode showed high concentration of inorganic fragments corresponding to where dendrites had formed, while intact areas remained clean [110]. Such chemical mapping confirms where dendrites travel in the microstructure. Moreover, ToF-SIMS can detect dopant or impurity migration; for instance, a fluorine-doped SSE was analyzed by ToF-SIMS which showed F distributed uniformly in the bulk of a fresh electrolyte but accumulated at the interface and within Li dendrites after cycling [111]. This suggested that F (from a LiF-based additive) migrated to form a protective layer *in situ*, consistent with its role in hindering dendrite growth. In summary, ToF-SIMS gives a 3D chemical view of dendrites and interphases, enabling researchers to trace dendrite pathways and identify elemental signatures of effective suppression (e.g., presence of certain elements along a blocked dendrite). Raman spectroscopy is a powerful tool to analyze both chemical species and mechanical strain in solid electrolytes. In the context of dendrite suppression,

Raman has been notably used for stress mapping inside SSEs. Because many ceramic electrolytes (like LLZO) have Raman-active lattice modes that shift under stress, confocal Raman microscopy can non-destructively probe internal stress distribution.

Hu et al. developed an advanced 3D confocal Raman microscopy method to map local mechanical stress in garnet-type LLZO solid electrolytes during lithium plating [112]. Their operando experiments revealed that lithium deposition induces substantial internal compressive stress—reaching up to ~1 GPa—especially near microstructural heterogeneities such as grain boundaries and pores. Crucially, Raman stress maps correlated these localized “hotspots” of stress with the post-mortem positions of dendritic filaments, confirming that non-uniform stress fields promote preferential dendrite nucleation [112]. This correlation is shown in Figure 4, where Raman-based stress distributions are directly compared with lithium deposition patterns, and supported by electro-chemo-mechanical modeling. The model explains how compressive stress raises the local chemical potential of lithium, increasing the overpotential for plating at specific sites and thereby driving heterogeneous dendrite growth [112]. Furthermore, their study demonstrated that stress distribution is not only induced during cycling but also heavily influenced by thermal history. Figure 4 integrates this insight by comparing LLZO pellets subjected to slow cooling versus rapid quenching [112]. The quenched sample exhibited much higher and more spatially heterogeneous compressive stresses, which correlate with a greater tendency toward dendrite penetration. Taken together, these results highlight that mechanical inhomogeneity—whether induced during fabrication or electrochemical operation—directly modulates the lithium deposition landscape. Strategies such as introducing compliant interlayers, controlling grain orientation, or applying uniform stack pressure could help redistribute internal stress and suppress dendrite initiation by flattening the overpotential landscape.

Raman spectroscopy is also employed to identify chemical compounds in the interphase; for instance, it can detect the formation of Li_2CO_3 or other crystalline reaction products on SSE surfaces [113]. These spectral signatures let researchers verify if, say, a CO_2 additive indeed produces a carbonate-based passivating layer, or if a sulfide SSE decomposes into sulfates or sulfides during cycling. Additionally, *in situ* Raman has been used in some studies to watch changes in polymer-based electrolytes or to monitor the consumption of additives that have distinct Raman peaks. Overall, Raman provides both a chemical fingerprint and a stress map, linking mechanical and chemical facets of dendrite suppression.

Nuclear Magnetic Resonance (NMR) spectroscopy (including magnetic resonance imaging, MRI) offers a unique bulk perspective, especially for quantifying lithium metal deposition and the formation of “dead” (electrically isolated) lithium. Because ^7Li is NMR-active, one can distinguish between Li in different environments (metallic lithium vs. ionic lithium in SSE vs. lithium in compounds) by their resonance shifts. Recent advances in operando NMR have enabled real-time quantification of lithium plating/stripping in solid-state cells. Maity et al. in 2023 used operando ^7Li NMR to monitor lithium in a symmetric cell with various sulfide electrolytes [114]. They could measure the growth of the Li metal signal during charging (plating) and how much of that lithium failed to be recovered on discharge, which corresponds to inactive Li. Impressively, by analyzing the NMR signal during resting periods, they found that mossy or dendritic lithium corrodes (reacts) faster than smoothly plated lithium in the cell [114]. In other words, a cell with rough, high-surface-area Li deposits lost NMR-visible Li signal more rapidly upon storage, indicating that dendritic Li was being consumed into inactive forms (like Li-S or Li-H compounds) much faster than a flat Li layer [114]. This quantification confirmed the intuition that dendrites not only risk short-circuiting but also exacerbate lithium consumption and capacity fade. Another cutting-edge study by Liang et al. [115] combined solid-state NMR

with Overhauser dynamic nuclear polarization (OE-DNP) to greatly boost sensitivity to the interfacial regions where dendrites and SEI form. This approach enabled unprecedented molecular-level insights into buried interphases without external spin labels. With DNP-enhanced NMR, they achieved molecular-level insight into composite polymer–ceramic electrolytes: they could detect small quantities of lithium species in the SEI and even measure how easily lithium ions moved through the SEI layer [115]. The authors quantitatively correlated ceramic content with dendrite quantity and cell lifetime, showing that 40 wt% ceramic loading offered optimal suppression, while higher filler contents (e.g., 60 wt%) impaired interfacial properties. They found that the quantity and penetration depth of dendrites depended on the ceramic filler content in the composite, correlating strongly with cell lifetime [115]. More importantly, they demonstrated that SEI signal enhancement in OE-DNP arises primarily from Li/Li⁺ charge transfer at the metal–SEI interface, rather than spin diffusion, allowing direct assessment of SEI lithium permeability. Moreover, by analyzing the NMR signal enhancements, they could directly determine the lithium permeability of the SEI, observing that certain interphase compositions allowed lithium-ion transport while blocking electron transport [115]. Through a combination of isotope enrichment, REDOR (Rotational-Echo Double Resonance) experiments, and CEST (Chemical Exchange Saturation Transfer) measurements, they showed that SEIs with similar chemical compositions (mainly Li₂O and LiOH) can exhibit markedly different ion permeabilities depending on their origin (polymer vs. ceramic). Figure 5 illustrates these findings, comparing chemical speciation, DNP-enhanced (Dynamic Nuclear Polarization-enhanced) NMR spectra signal strength, and electron microscopy data for SEIs formed with increasing ceramic content. This kind of information is invaluable—it tells us how effective a tailored SEI or artificial interphase is at stopping dendrites (which require electronic connectivity to keep growing) while still permitting ionic flow. These findings not only elucidate how SEI architecture and ceramic fillers affect dendrite suppression, but also establish OE-DNP as a powerful diagnostic tool to assess the functional quality of SEIs in solid-state batteries. As NMR techniques continue to advance (with higher fields, better probes, and DNP), we expect even more quantitative understanding of dendrite suppression, such as measuring how much lithium becomes “dead” in different cell configurations or how fast dendrites grow inside an opaque SSE.

X-ray diffraction (XRD) is a fundamental technique for characterizing the crystal structure, phase composition, and lattice parameters of both solid electrolytes and electrode materials in solid-state lithium batteries (SSLBs). It plays a crucial role in identifying structural changes that occur during lithium plating/stripping cycles, particularly those related to dendrite formation. While conventional laboratory-based XRD is effective for ex situ structural analysis, synchrotron-based XRD offers significantly higher resolution, sensitivity, and temporal resolution, enabling operando or in situ monitoring of phase transformations and interfacial reactions at the electrode–electrolyte interface. Recent studies have demonstrated the use of synchrotron XRD to detect the nucleation and growth of lithium dendrites in real time, providing insights into their crystalline nature and the stress-induced distortions they cause in solid electrolytes [116]. For instance, researchers have used operando synchrotron XRD to monitor phase evolution in sulfide-based SSEs during battery cycling, revealing the onset of interfacial degradation and lithium filament growth before cell failure [117]. Similarly, Duan et al. applied synchrotron diffraction to examine the effect of external pressure on suppressing dendrites in oxide-based electrolytes, highlighting the importance of mechanical constraints on structural integrity [118]. Moreover, synchrotron microdiffraction techniques have enabled spatially resolved mapping of stress fields and microcracks associated with dendrite-induced damage [119]. The integration of synchrotron XRD with complementary techniques, such as X-ray absorption

spectroscopy (XAS) or X-ray computed tomography (XCT), further enriches the understanding of degradation mechanisms and guides the rational design of dendrite-tolerant materials. As such, synchrotron-based diffraction has become an indispensable tool in the real-time structural monitoring of SSLBs, contributing directly to the development of safer and longer-lasting devices.

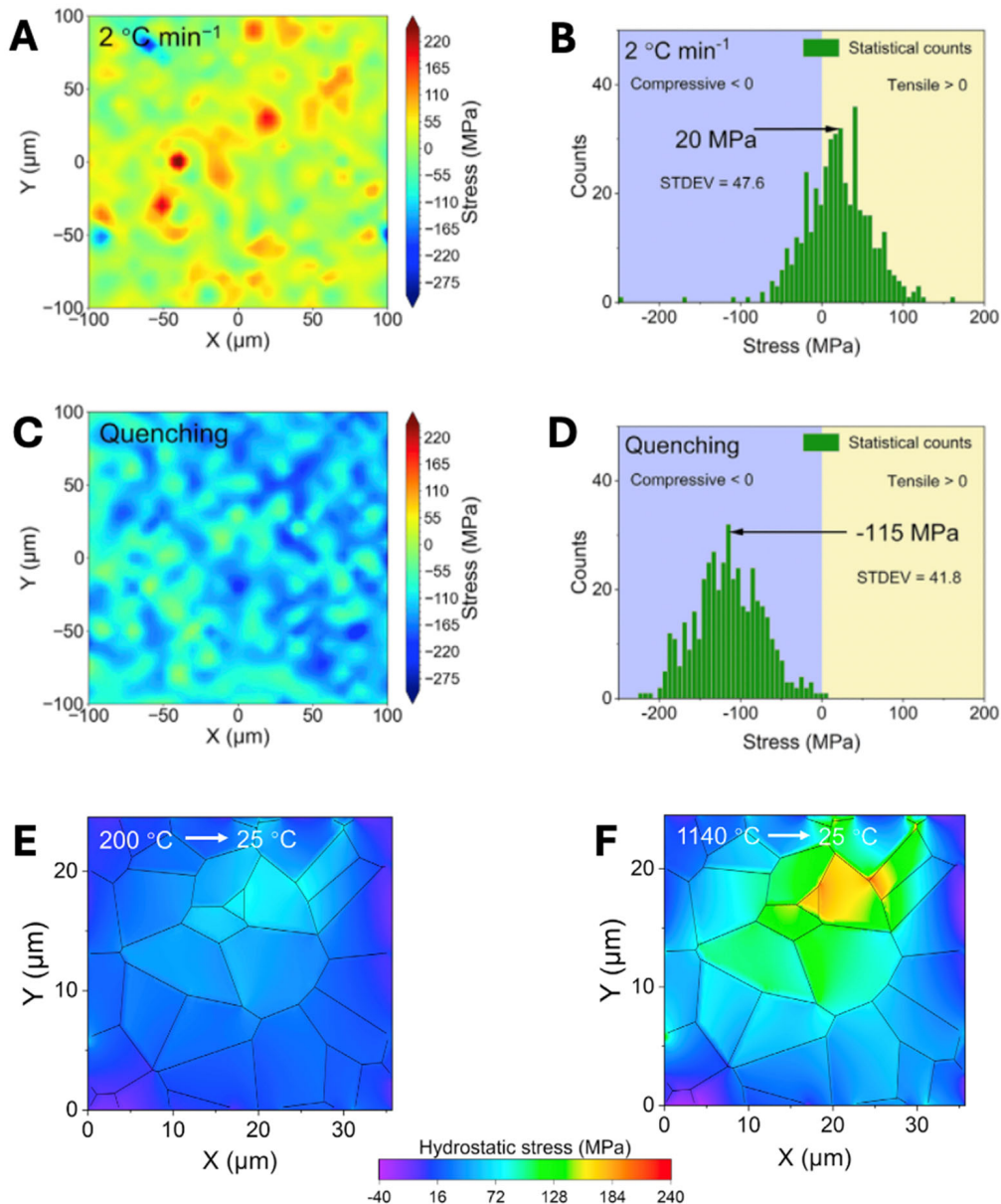


Figure 4. Correlation between local compressive stress and dendrite formation in LLZO during Li plating, mapped via 3D confocal Raman microscopy. (A,B) Mapped stress distribution and statistical stress profile of a LLZTO pellet cooled slowly from 1140 °C to room temperature at a rate of 2 °C/min, showing relatively low and uniform tensile stresses across a 200 × 200 μm area. (C,D) Stress map and analysis for a similar pellet subjected to rapid quenching, revealing pronounced spatial heterogeneity and significantly higher compressive stresses. (E) Hydrostatic stress distribution in an LLZO sample cooled rapidly from 200 °C to room temperature, showing moderate stress levels (median ~22 MPa) but noticeable spatial variation of up to 102 MPa across the region. (F) Hydrostatic stress distribution in a sample quenched from 1140 °C reveals much stronger inhomogeneity, with high-stress zones localized at triple grain junctions. The median stress increases to ~50 MPa, and local differences reach up to 235 MPa across the sample. (Adapted with permission from ref. [112], Cell Press 2022).

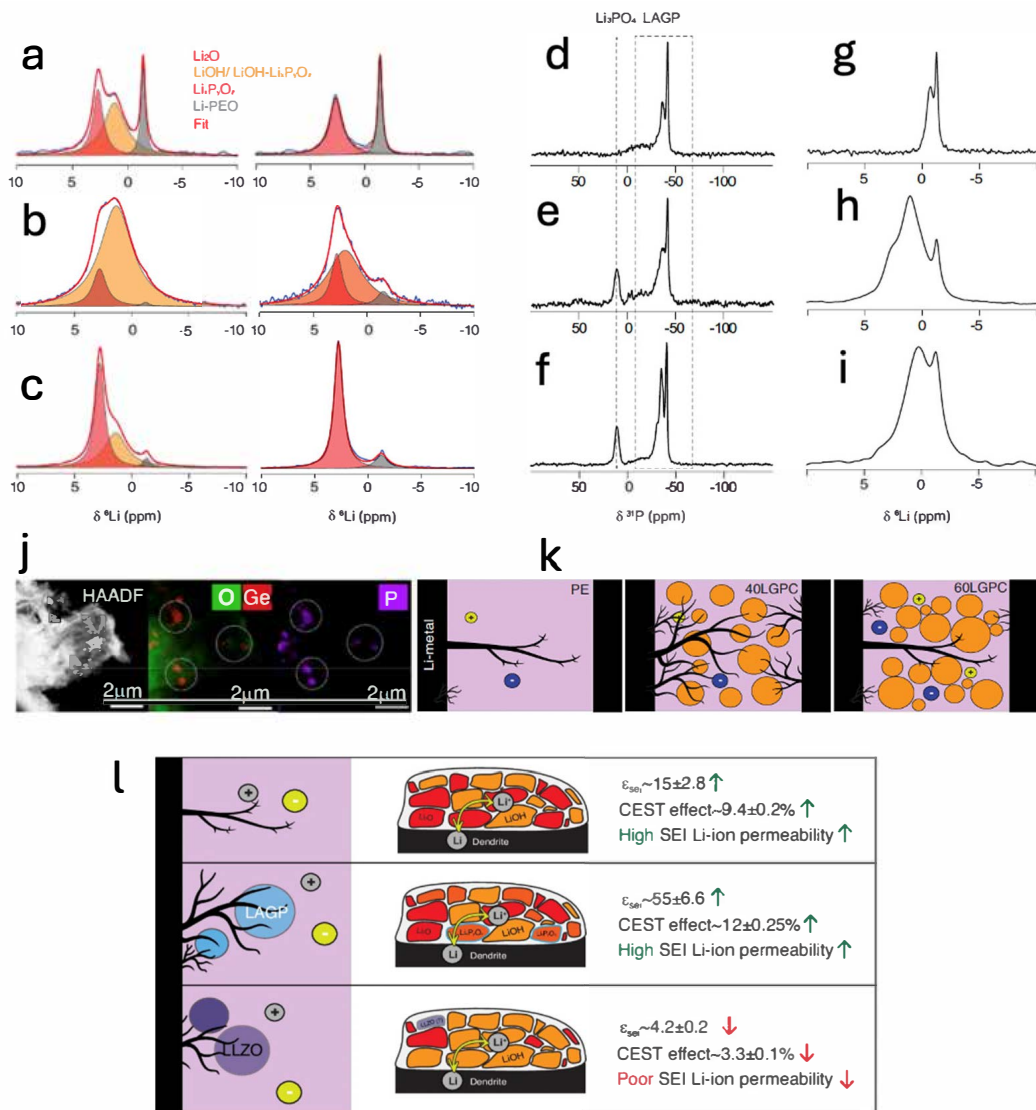


Figure 5. DNP-enhanced (Dynamic Nuclear Polarization-enhanced) NMR spectra and HAADF-STEM analysis of SEI composition and lithium dendrite suppression in polymer–ceramic composite electrolytes. (a–c) ${}^6\text{Li}$ MAS NMR spectra deconvoluted into Li_2O , $\text{LiOH}/\text{LiOH}\text{-Li}_3\text{PO}_4$, and Li-PEO species across PE, 40LGPC, and 60LGPC compositions. (d–f) ${}^{31}\text{P}$ MAS NMR spectra showing signals from Li_3PO_4 and LAGP. (g–i) DNP-enhanced ${}^6\text{Li}$ NMR showing signal amplification near the Li/SEI interface. (j) HAADF-STEM and EDX maps of O, Ge, and P revealing interphase structure. (k) Schematic representations of dendrite behavior under different ceramic loadings: unrestricted in PE, blocked in 60LGPC. (l) Diagram illustrating the relationship between SEI composition and Li^+ transport properties as influenced by varying ceramic content, derived from CEST analysis and Overhauser-enhanced DNP measurements. (Adapted with permission from ref. [115], Springer Nature 2024).

Finally, electrochemical impedance spectroscopy (EIS), though not a spectroscopy of photons or particles, is a frequency-domain characterization technique often classified among spectroscopic methods for batteries. In the context of dendrites, EIS is a crucial operando tool to detect interface degradation and incipient shorts [109,120]. A rising interfacial resistance or the appearance of an additional low-frequency semicircle in an EIS spectrum can indicate the build-up of a resistive SEI or the formation of voids, while a sudden drop in impedance (especially in combination with a cell voltage plunge) often signifies an internal short by a dendrite. Researchers frequently couple EIS with the aforementioned methods: for instance, Huo et al. [107] performed time-dependent EIS alongside in situ XPS to show that the LiF-rich interface not only existed (by XPS) but

also maintained low impedance over time (by EIS), correlating with stable cycling without dendrites. Likewise, in operando NMR studies, EIS can track when a cell approaching failure exhibits a drop in charge transfer resistance, aligning with the NMR's detection of increasing "dead" lithium. In a 2022 report, Gao et al. [105] noted that under strong mechanical confinement, the EIS of a Li|LLZO cell remained stable (no new interfacial arc) as lithium plated laterally, but when a vertical dendrite burst through, the cell's impedance suddenly collapsed, reflecting the short-circuit path formed [105]. Such observations reinforce that impedance changes can serve as early warning signs of dendrite formation. Moreover, EIS is invaluable for evaluating suppression strategies: a successful strategy (e.g., a doped SSE or a protective layer) should raise the critical current density at which the impedance catastrophically drops (i.e., it delays the dendrite-induced short). Thus, many researchers report improved EIS stability or higher post-cycling impedance retention as evidence of suppressed dendrite growth [107]. While EIS alone cannot visualize dendrites, when interpreted alongside physical characterization it provides a quantitative measure of interfacial stability and ion transport over the course of cycling. In summary, advanced spectroscopic techniques offer deep insights into why and how certain interfacial engineering approaches work to suppress dendrites. XPS and ToF-SIMS reveal the chemical makeup and distribution of critical interphase layers (e.g., confirming the presence of a dendrite-blocking LiF/Li₂S layer or detecting unwanted metallic Li percolation). Raman spectroscopy links mechanical stress and dendrite growth, guiding mechanical mitigation strategies. NMR directly quantifies dendritic lithium and inactive lithium, informing how much of the anode is effectively lost to side reactions and how different designs minimize that loss. EIS ties it all together by indicating the electrochemical stability of the interface throughout cycling. Together with *in situ* electron microscopy, these spectroscopic methods form a powerful toolkit. By applying multiple characterization techniques in tandem, researchers can observe dendrites forming (or being suppressed) in real time, identify the chemical and mechanical state of the interface, and correlate those findings with battery performance. This comprehensive understanding is driving rational design of solid-state batteries—for example, choosing dopants that create favorable interphase chemistry (as verified by XPS/NMR) or engineering flexible yet robust interfaces that relieve stress (as evidenced by Raman/SEM)—ultimately pushing the field closer to dendrite-proof, high-performance all-solid-state lithium batteries.

4. Conclusions and Future Perspectives

Solid-state lithium metal batteries (SSLBs) have seen rapid progress in strategies to combat lithium dendrites, which remain the primary roadblock to their reliability and commercialization [113,121]. A plethora of interface engineering approaches and material innovations have been explored to suppress dendrite initiation and propagation. On the interface side, researchers have designed artificial interphases and interlayers to stabilize the Li metal/SSE (solid-state electrolyte) contact. For example, Wan et al. introduced a mixed ionic–electronic conductive interlayer that reacts *in situ* to form a multiphase solid interphase (containing LiMgS_x, porous LiH–Li₃N, and a Li–Mg–La alloy) [122]. This interphase increased the critical interphase overpotential (CIOP)—a new figure of merit for dendrite resistance—from ~10 mV for a bare Li₆PS₅Cl electrolyte to ~220 mV [122]. Such a dramatic enhancement means the solid electrolyte can sustain much higher current before dendrites nucleate, by virtue of an interphase that is mechanically robust, lithiophobic, and optimally conductive [122]. Material innovations in electrolytes have been equally critical. High-modulus ceramic electrolytes (e.g., oxides like LLZO or sulfides like Li₁₀GeP₂S₁₂) [123] were initially expected to block dendrites thanks to their stiffness. However, in practice even these "hard" electrolytes suffer dendrite penetration along microstructural weak-

nesses such as grain boundaries and defects [121]. This has prompted the development of advanced electrolyte architectures: examples include amorphous or nanocrystalline electrolytes with no grain boundaries (which showed dendrite-free operation up to mA cm⁻² level currents) [70], and composite electrolytes where a secondary phase is embedded to redirect or blunt dendrite growth. Phase-field modeling by Yuan et al. demonstrates that incorporating “brick-and-mortar” style heterogeneous reinforcements within a brittle electrolyte can divert lithium filaments and prevent internal short-circuiting [124]. Similarly, multi-layered electrolyte designs have proven effective: Hu et al. showed that even if a dendrite begins to form, a multi-layer stack of differing materials (e.g., Li₆PS₅Cl—Li₃ScCl₆—Li₆PS₅Cl) causes the dendritic crack to deflect at the layer interfaces, rather than puncturing straight through [125]. This crack-deflection mechanism can substantially raise the effective critical current density by forcing the dendrite to travel laterally, increasing the path length and resistance [125]. In essence, today’s dendrite suppression toolkit spans chemical interphase design, microstructural engineering, and mechanical modulation, each contributing to a more uniform and resilient Li plating/stripping behavior.

Despite these encouraging strategies, achieving a truly dendrite-proof solid-state battery under practical conditions remains an unsolved challenge. A critical assessment reveals several persistent limitations. First, many suppression methods succeed only under limited conditions (e.g., small cell prototypes, moderate current densities, or with external pressure). Dendrites can still emerge if the system is pushed towards EV-level fast-charge currents or long cycle counts. Recent operando studies have exposed the nuanced failure modes—initiation vs. propagation—of dendrites in SSEs. Ning et al. demonstrated that lithium filament initiation often starts at microscopic defects: Li metal can infiltrate pre-existing pores or microcracks at the Li/SSE interface, nucleating a subsurface dendrite [126]. Such initiation is governed by local features like grain boundary fracture strength, defect size, and local current hot-spots [126]. Once a filament has nucleated, its *propagation* through the electrolyte is controlled by more macroscopic factors: the bulk fracture toughness of the SSE, the length of the growing Li filament, the applied stack pressure, and cycling depth [126]. This dichotomy means a successful suppression strategy must address both the microscale interface flaws (to avoid initial “seed” formation) and the bulk propagation (to arrest any filament that does start). For instance, even the hardest ceramics (garnets, etc.) are not immune—tiny grain boundary gaps or electronic percolation paths can enable a dendrite to start, and high stack pressure (initially applied to ensure contact) can actually drive a crack forward once initiated [126]. Indeed, counterintuitively, Ning et al. observed that lowering stack pressure after dendrite initiation suppressed crack propagation and extended cell life [126]. This highlights the complexity of mechanical influences and the need for “smart” pressure management during operation. Another major challenge is the formation of Li voids and interface gaps during cycling. When lithium strips from the anode, voids can form at the Li/SSE interface if ion transport and Li deposition are uneven, leading to loss of contact and non-uniform current distribution. These voids then become hotspots for dendrite re-nucleation in subsequent plating. Recent research in *Joule* showed that regulating lithium diffusion to suppress void formation dramatically improved interface stability and delayed dendrite onset [127]. However, eliminating voids in a practical cell (which undergoes thousands of cycles and varying duty conditions) is extremely difficult. Chemical compatibility issues also exacerbate dendrite problems: if the Li metal aggressively reacts with the electrolyte, the resulting interphase can be mechanically weak or electronically conductive, both of which encourage dendrites. Sulfide electrolytes, for example, have superb ionic conductivity but tend to form reduced interphases (e.g., Li₂S or Li-In alloys) that may not effectively passivate the lithium surface [121]. While protective coating layers (LiI, LiF, polymer buffers, etc.) have been used to mitigate this,

maintaining a stable, long-lived interphase is nontrivial, especially over broad temperature and current ranges.

From an engineering standpoint, manufacturability and scaling impose further constraints. Many of the laboratory demonstrations (e.g., ultrathin amorphous films, multi-layer ceramics, high-pressure cells) are difficult to translate to mass production. Creating large-area, defect-free solid electrolyte membranes is a formidable task—even tiny defects can trigger dendrites, yet completely eliminating defects in a $>100\text{ }\mu\text{m}$ thick, brittle ceramic separator over square-meter areas is nearly impossible with current techniques [121]. Present solid electrolytes often require high temperature sintering or careful air-free processing; producing them in high volume with consistent quality is a challenge. In summary, today's dendrite suppression strategies, while greatly advanced, have not fully conquered the unpredictable nature of Li dendrites under real-world conditions. Improvements tend to be incremental, and a holistic solution is still lacking.

Looking ahead, several research directions are paramount to achieving dendrite-free SSLBs. At the materials level, one priority is the development of strong yet deformable solid electrolytes that combine high ionic conductivity with excellent toughness and self-adaptivity. This might involve composite designs that marry ceramics for stiffness with polymers for elasticity, so that the electrolyte can accommodate stress without cracking. Enhancing the fracture toughness of brittle inorganic SSEs (for example, through grain boundary engineering, second-phase toughening, or even leveraging polymer-inorganic hybrids) could prevent crack initiation and propagation by lithium filaments. There is growing interest in single-crystal or texturized ceramic electrolytes—by eliminating or aligning grain boundaries, dendrite pathways may be minimized. Parallel to that, glassy or amorphous electrolytes (which inherently lack grain boundaries) are being revisited; their historically lower ionic conductivities are now improving, and their uniform structure offers potential dendrite resistance [70]. Another promising materials approach is using self-healing or adaptive components: for instance, electrolytes containing nanosized piezoelectric or ferroelectric particles that generate local stress under an electric field, actively counteracting dendrite growth forces [128,129]. Preliminary simulations suggest a piezoelectric-infused electrolyte can dynamically suppress dendrite driving force at high current by redistributing mechanical stress [128]—this kind of “active” dendrite prevention could be revolutionary if realized experimentally. Interface-focused research remains crucial as well. The ideal Li/electrolyte interface should promote uniform Li plating/stripping and remain intimately contacted over many cycles. Future studies are likely to explore artificial interphases that are pre-engineered at the molecular level—for example, thin lithiophilic layers that ensure initial wetting and plating uniformity, coupled with lithiophobic, stiff layers that repel lithium from certain regions to prevent filament intrusion [130]. Novel interphase chemistries (e.g., based on nitrides, halides, or 2D materials) are being investigated to combine high ionic conductivity with electronic insulation and mechanical strength. In situ interface formation is another priority: one strategy is to use a slight prelithiation of a solid electrolyte or a sacrificial layer that reacts with Li on first contact to form a stable, dendrite-suppressing interphase in operando [122]. By tailoring the composition (for instance, incorporating elements that form strong ceramic phases like LiF, Li₃N, or Li₂O at the interface), the community aims to create self-passivating interfaces analogous to the SEI in liquid cells, but optimized for solids. Additionally, management of the Li deposition morphology via current modulation is an emerging research frontier. Applying pulse charging or alternating plating/stripping protocols can allow the Li surface to “relax” and redistribute, potentially avoiding runaway dendrite growth—early reports show that such electrochemical control can delay dendrite formation in solid cells [131].

These electrochemically driven approaches will benefit from further fundamental studies linking ionic transport kinetics with interface stability.

Equally important is a mechanistic understanding that bridges nano-scale processes to macro-scale cell behavior. The community is increasingly combining advanced characterization (e.g., synchrotron X-ray tomography, electron microscopy, and micro-Raman mapping) with simulation (e.g., molecular dynamics and phase-field models) to visualize how and where dendrites form inside SSEs [16]. For instance, a recent atomic-scale simulation by Zhang et al. reproduced dendrite penetration in a ceramic and confirmed that classic fracture mechanics (Griffith's criteria) apply at the Li tip, but with an electrochemical twist: high local Li^+ concentration can reduce the ceramic's fracture toughness [16]. Such insights imply that dendrite suppression may require both mechanical fortification and local chemical conditioning of the electrolyte. Future research will likely prioritize *grain boundary modifications* (to reduce electronic leakage and increase toughness at those critical interfaces) and *space-charge layer engineering* (using space-charge effects to distribute Li deposition more uniformly). In summary, research efforts must become more cross-disciplinary—incorporating mechanics, materials science, and electrochemistry—to converge on robust solutions. Every element of the cell, from the atomic lattice of the electrolyte to the external stack pressure, plays a role in dendrite behavior, so the next breakthroughs will stem from unifying these perspectives.

Achieving dendrite-free solid-state batteries is not only a scientific quest but also an engineering challenge of integration, scalability, and cost. From an industrial standpoint, the path forward will require translating lab-scale innovations into manufacturable components. One key consideration is electrolyte thickness and cell architecture. Presently, many ceramic SSEs need to be on the order of hundreds of microns thick to prevent mechanical failure, yet this severely penalizes energy density and increases resistance [121]. A major technical goal is to produce thin (tens of μm) electrolyte membranes that are mechanically robust over large areas. This might involve new fabrication techniques such as tape-casting, roll-pressing, or even glass-forming methods to create thin, defect-minimized sheets. Simultaneously, cell stacking designs must accommodate solid components—unlike liquid cells that tolerate some swelling, SSLB stacks must maintain contact at every interface. Innovative engineering like spring-loaded or flexible stack frames, as well as heat/pressure management systems, may be incorporated to keep cells under just the right pressure (not too high to drive dendrites, but enough to ensure contact) based on the recent understanding of pressure effects [126]. In terms of integration routes, hybrid approaches are likely to serve as interim solutions on the way to fully solid-state batteries. We may see “quasi-solid” batteries where a thin layer of gel or polymer is used at the interface to alleviate contact issues and heal minor defects, effectively combining the advantages of liquid and solid electrolytes [132]. This could allow earlier commercialization by leveraging existing lithium-ion manufacturing infrastructure (coating, lamination techniques) while incrementally improving safety and dendrite resistance. Indeed, some startups and automakers are pursuing composite electrolyte designs (ceramic particles in polymer matrices) as they are more immediately scalable—these can be made using roll-to-roll processes similar to current separators, potentially lowering the barrier to entry. The economic feasibility of SSLBs will depend heavily on such manufacturability. Current solid electrolytes involve costly materials (e.g., lanthanum, germanium, indium in LLZO or LGPS) and sensitive processing (air-free handling for sulfides, high-temperature sintering for oxides) [121]. To reach cost parity with conventional batteries, research is needed on low-cost material alternatives (for instance, halide electrolytes that avoid expensive rare-earths, or novel polymer–ceramic hybrids using abundant elements) and on streamlining the fabrication process. Encouragingly, there is progress in wet-chemical synthesis of sulfide electrolytes at scale and in sintering

techniques that use lower temperatures or even pressureless sintering, which could cut production time and cost [121]. Moreover, as solid-state technology matures, economies of scale and supply chain development (for SSE powders, Li metal foils, etc.) will drive down costs. Industry roadmaps suggest that if technical hurdles (dendrites, interface resistance, etc.) are cleared in the next few years, pilot production lines could ramp up such that solid-state EV batteries might approach competitive cost-per-kWh by the late 2020s.

Another aspect of commercial readiness is how dendrite-free SSLBs integrate into full battery packs and systems. Manufacturers must consider how to monitor and ensure long-term stability of each cell in a pack. Traditional BMSs (battery management systems) may need to evolve to detect early signs of dendritic failure (for example, using voltage noise analysis or pressure sensors, since a dendrite in a solid cell might produce a subtle signal before shorting). The safety advantages of solid electrolytes—non-flammability and resistance to dendrite-induced thermal runaway—are a major driving force for commercialization [132]. If SSLBs can be truly dendrite-free, the risk of internal short and fire is drastically reduced, making them highly attractive for electric vehicles and grid storage in terms of safety. However, it is worth noting that dendrite suppression alone does not guarantee a flawless battery: issues like cathode interface degradation, manufacturing defects, or thermal stress can also cause failures. Thus, a *dendrite-free SSLB* must be designed in concert with robust cathode interfaces and overall cell engineering. Pilot projects are already testing solid-state cells in modules under real-world conditions (varying temperatures, fast charging, crash safety, etc.). These early trials will inform necessary design tweaks—for instance, whether additional protective circuits are needed or if the solid cells indeed prevent the kind of cascading failures seen in Li-ion packs. Achieving a commercially viable, dendrite-free SSLB will likely proceed in phases. The near-term goal (next 2–3 years) is demonstrating mid-size cells (several Ah capacity) that can cycle hundreds of times at reasonable currents without dendrite-induced failure. Success here would rely on implementing the best current strategies (optimized interlayers, high-quality SSE membranes, controlled pressure) in a scaled format. Collaboration between academia and industry is accelerating this step—for example, consortia are sharing insights on fabrication and testing protocols for solid-state cells. The medium-term goal (3–5 years) focuses on process optimization and up-scaling: refining manufacturing methods to consistently produce dendrite-resistant cells in high volume and yield. During this period, we may see the first niche commercial products using SSLBs (e.g., in consumer electronics or as auxiliary power units in luxury vehicles) where the high cost is offset by premium performance or safety. These early products will validate the technology in the field and likely use conservative designs (perhaps slightly thicker electrolytes or lower-charge protocols) to ensure no dendrite failures, while the technology is still being perfected. The long-term vision is that within a decade, dendrite-free solid-state batteries could penetrate mainstream EV markets, offering higher energy density and improved safety over current Li-ion batteries. To realize this, all the pieces must come together: materials that inherently prevent dendrites, interfaces that remain stable over thousands of cycles, and manufacturing that delivers this reliability at scale and at an acceptable cost.

In summary, while formidable challenges remain, the field has made clear strides toward understanding and suppressing dendrites in solid-state batteries. Each incremental advance—be it a new interfacial coating that boosts the critical current, or a novel electrolyte that resists fracture—builds confidence that dendrites can ultimately be tamed. The consensus in recent high-impact studies is that no single silver bullet exists; instead, a holistic engineering of materials, interfaces, and cell design is required [132]. The ongoing convergence of fundamental insights and innovative engineering gives a strategic pathway forward. By prioritizing defect-free electrolyte fabrication, self-forming stable interfaces,

and smart mechanical design, researchers are actively removing the barriers one by one. The coming years will be pivotal: as research priorities align with industrial feasibility, we move steadily closer to commercializing dendrite-free solid-state lithium batteries—a technology that promises to revolutionize energy storage with greater safety and energy density. The lessons learned in this quest will not only enable SSLBs but also enrich the broader understanding of electrochemical interfaces and fracture, benefiting the battery field. There is optimism that the advances in dendrite suppression, from interface engineering to material innovation, will coalesce to deliver solid-state batteries that meet the stringent requirements of real-world applications, ushering in a new era of energy storage.

Technological and Commercial Outlook (Summary): Integration Routes: Hybrid solid-liquid designs may bridge the gap initially, but the goal is fully solid cells with thin, robust electrolytes and scalable manufacturing. **Economic Feasibility:** Costs remain higher than incumbent Li-ion technology due to expensive materials and processing, but innovations in materials (e.g., replacing costly elements) and process (simplified synthesis, roll-to-roll production) are actively reducing these barriers [133]. With increasing investment and pilot production lines, the economies of scale are expected to improve—recent analyses project that if challenges are overcome, solid-state EV batteries could reach competitive cost levels in the late 2020s. **Industry-Readiness:** Several automotive OEMs and battery startups report achieving milestone demonstrations (hundreds of cycles, moderate fast-charge) with prototype solid-state cells. However, to be industry-ready, these cells must prove reliable dendrite-free performance in multi-cell modules under diverse conditions. The next few years will likely see rapid progress in this area, guided by the research breakthroughs in dendrite suppression. The strategic vision is that through continued interdisciplinary innovation, dendrite-free solid-state lithium batteries will move from laboratories to factories, enabling safer and more powerful energy storage systems for our electrified future. A projected roadmap summarizing the key developmental milestones is shown in Figure 6.

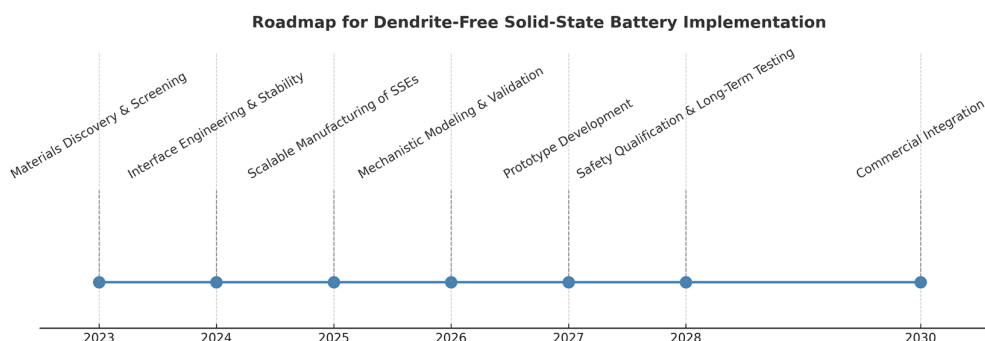


Figure 6. Roadmap outlining critical stages toward the implementation of dendrite-free solid-state lithium batteries (SSLBs). Early-stage activities—including materials discovery, interface stabilization, and the scalable processing of solid-state electrolytes (SSEs)—are already underway or progressing significantly as of 2025. Subsequent phases, such as mechanistic validation, prototype development, and long-term safety testing, will be critical to achieve commercial integration by the end of the decade.

Author Contributions: Conceptualization, F.M. and A.M.; methodology, F.M.; formal analysis, A.M. and F.M.; investigation, A.M., M.C.C., F.D., J.D. and F.M.; resources, A.M., M.C.C., F.D., J.D. and F.M.; writing—original draft preparation, A.M., M.C.C., F.D., J.D. and F.M.; writing—review and editing, A.M., F.M., M.C.C., J.D. and F.D.; supervision, F.M.; project administration, F.M.; funding acquisition, F.M., A.M., F.D., J.D. and M.C.C. All authors have read and agreed to the published version of the manuscript.

Funding: Financial support from NSF Center for the Advancement of Wearable Technologies-CAWT (Grant 1849243) and from the Consortium of Hybrid Resilient Energy Systems CHRES (DE-NA0003982) are gratefully acknowledged.

Institutional Review Board Statement: Not applicable.

Informed Consent Statement: Not applicable.

Data Availability Statement: The data is contained in the article and is available from the corresponding authors on reasonable request.

Acknowledgments: The authors gratefully acknowledge Raúl S. García, Dina Márquez, and Dock García for their valuable assistance in organizing and updating the research databases, as well as for their support in coordinating the bibliography.

Conflicts of Interest: The authors declare no conflicts of interest.

Abbreviations

The following abbreviations are used in this manuscript:

AFM	Atomic Force Microscopy
ALD	Atomic Layer Deposition
ASSLBs	All-Solid-State Lithium Batteries
DFT	Density Functional Theory
EIS	Electrochemical Impedance Spectroscopy
ETEM	Environmental Transmission Electron Microscopy
FEC	Fluoroethylene Carbonate
GCSE	Gradient Composite Solid Electrolyte
GO	Graphene Oxide
LLZO	$\text{Li}_7\text{La}_3\text{Zr}_2\text{O}_{12}$
LATP	Li-Al-Ti-P oxide
LFP	LiFePO_4
LiTFSI	Lithium bis(trifluoromethanesulfonyl)imide
LLZTO	$\text{Li}_{6.4}\text{La}_3\text{Zr}_{1.4}\text{Ta}_{0.6}\text{O}_{12}$
LIBs	Lithium-Ion Batteries
LiPON	Lithium Phosphorus Oxynitride
MRI	Magnetic Resonance Imaging
MPa	Megapascal
MoS ₂	Molybdenum Disulfide
NCM811	$\text{LiNi}_{0.8}\text{Co}_{0.1}\text{Mn}_{0.1}\text{O}_2$
NMR	Nuclear Magnetic Resonance
PEO	Polyethylene Oxide
PSE	Polymer-Based Solid Electrolytes
PVDF-TrFE	Poly(vinylidene fluoride-co-trifluoroethylene)
rGO	Reduced Graphene Oxide
SEI	Solid Electrolyte Interphase
SEM	Scanning Electron Microscopy
SHE	Standard Hydrogen Electrode
SSE	Solid-State Electrolyte
SSLBs	Solid-State Lithium Batteries
TEM	Transmission Electron Microscopy
ToF-SIMS	Time-of-Flight Secondary Ion Mass Spectrometry
XPS	X-ray Photoelectron Spectroscopy

References

- Albertus, P.; Babinec, S.; Litzelman, S.; Newman, A. Status and Challenges in Enabling the Lithium Metal Electrode for High-Energy and Low-Cost Rechargeable Batteries. *Nat. Energy* **2017**, *3*, 16–21. [[CrossRef](#)]
- Janek, J.; Zeier, W.G. A Solid Future for Battery Development. *Nat. Energy* **2016**, *1*, 16141. [[CrossRef](#)]
- Goodenough, J.B.; Singh, P. Review—Solid Electrolytes in Rechargeable Electrochemical Cells. *J. Electrochem. Soc.* **2015**, *162*, A2387–A2392. [[CrossRef](#)]
- Famprikis, T.; Canepa, P.; Dawson, J.A.; Islam, M.S.; Masquelier, C. Fundamentals of Inorganic Solid-State Electrolytes for Batteries. *Nat. Mater.* **2019**, *18*, 1278–1291. [[CrossRef](#)] [[PubMed](#)]
- Kerman, K.; Luntz, A.; Viswanathan, V.; Chiang, Y.-M.; Chen, Z. Review—Practical Challenges Hindering the Development of Solid State Li Ion Batteries. *J. Electrochem. Soc.* **2017**, *164*, A1731–A1744. [[CrossRef](#)]
- Nzereogu, P.U.; Oyesanya, A.; Ogba, S.N.; Ayanwunmi, S.O.; Sobajo, M.S.; Chimsunum, V.C.; Ayanwunmi, V.O.; Amoo, M.O.; Adefemi, O.T.; Chukwudi, C.C. Solid-State Lithium-Ion Battery Electrolytes: Revolutionizing Energy Density and Safety. *Hybrid. Adv.* **2025**, *8*, 100339. [[CrossRef](#)]
- Li, Y.; Kim, C.; Cho, Y.; Musgrave, A.L.; Parker, G.D.; Su, Y.-F.; Sacci, R.L.; Yu, X.-Y.; Zawodzinski, T.; Nanda, J.; et al. Promising Performance of Sulfide Catholytes Compared to Halide Alternatives in NMC811 Cathodes for Sheet-Type Sulfide Solid-State Batteries. *Energy Storage Mater.* **2025**, *80*, 104385. [[CrossRef](#)]
- Maurel, A.; Armand, M.; Gruegeon, S.; Fleutot, B.; Davoisne, C.; Tortajada, H.; Courty, M.; Panier, S.; Dupont, L. Poly(Ethylene Oxide)—LiTFSI Solid Polymer Electrolyte Filaments for Fused Deposition Modeling Three-Dimensional Printing. *J. Electrochem. Soc.* **2020**, *167*, 070536. [[CrossRef](#)]
- Mindemark, J.; Lacey, M.J.; Bowden, T.; Brandell, D. Beyond PEO—Alternative Host Materials for Li⁺—Conducting Solid Polymer Electrolytes. *Prog. Polym. Sci.* **2018**, *81*, 114–143. [[CrossRef](#)]
- Zhu, Y.; He, X.; Mo, Y. First principles study on electrochemical and chemical stability of solid electrolyte–electrode interfaces in all-solid-state Li-ion batteries. *J. Mater. Chem. A* **2016**, *4*, 3253–3266. [[CrossRef](#)]
- Zhang, Z.; Shao, Y.; Lotsch, B.; Hu, Y.-S.; Li, H.; Janek, J.; Nazar, L.F.; Nan, C.-W.; Maier, J.; Armand, M.; et al. New Horizons for Inorganic Solid State Ion Conductors. *Energy Environ. Sci.* **2018**, *11*, 1945–1976. [[CrossRef](#)]
- Wang, C.; Fu, K.; Kammampata, S.P.; McOwen, D.W.; Samson, A.J.; Zhang, L.; Hitz, G.T.; Nolan, A.M.; Wachsman, E.D.; Mo, Y.; et al. Garnet-Type Solid-State Electrolytes: Materials, Interfaces, and Batteries. *Chem. Rev.* **2020**, *120*, 4257–4300. [[CrossRef](#)] [[PubMed](#)]
- Burton, M.; Narayanan, S.; Jagger, B.; Olbrich, L.F.; Dhir, S.; Shibata, M.; Lain, M.J.; Astbury, R.; Butcher, N.; Copley, M.; et al. Techno-Economic Assessment of Thin Lithium Metal Anodes for Solid-State Batteries. *Nat. Energy* **2024**, *10*, 135–147. [[CrossRef](#)]
- Machín, A.; Morant, C.; Márquez, F. Advancements and Challenges in Solid-State Battery Technology: An In-Depth Review of Solid Electrolytes and Anode Innovations. *Batteries* **2024**, *10*, 29. [[CrossRef](#)]
- Ningappa, N.G.; Vishweswariah, K.; Bouguern, M.D.; Anil Kumar, M.R.; Amine, K.; Zaghib, K. Mechanistic Insights and Materials Strategies for Dendrite-Free Metal Anodes in Alkali and Zinc Batteries. *Nano Energy* **2025**, *141*, 111144. [[CrossRef](#)]
- Zhang, B.; Yuan, B.; Yan, X.; Han, X.; Zhang, J.; Tan, H.; Wang, C.; Yan, P.; Gao, H.; Liu, Y. Atomic Mechanism of Lithium Dendrite Penetration in Solid Electrolytes. *Nat. Commun.* **2025**, *16*, 1906. [[CrossRef](#)]
- An, Y.; Hu, T.; Pang, Q.; Xu, S. Observing Li Nucleation at Li Metal–Solid Electrolyte Interface in All-Solid-State Batteries. *arXiv* **2024**, arXiv:2412.12611. [[CrossRef](#)]
- Guo, W.; Wang, A.; He, X.; Lei, Y.; Li, Y.; Zhou, Z.; Li, C.; Lv, X.; Wang, H.; Shen, F.; et al. Unveiling the Mechanism of Lithium Dendrite Infiltration into Solid State Electrolyte through the Coupling of Electrochemical and In-Situ Optical Characterization. *Electrochim. Acta* **2024**, *508*, 145294. [[CrossRef](#)]
- Liu, H.; Chen, Y.; Chien, P.-H.; Amouzandeh, G.; Hou, D.; Truong, E.; Oyekunle, I.P.; Bhagu, J.; Holder, S.W.; Xiong, H.; et al. Dendrite Formation in Solid-State Batteries Arising from Lithium Plating and Electrolyte Reduction. *Nat. Mater.* **2025**, *24*, 581–588. [[CrossRef](#)]
- Yildirim, C.; Flatscher, F.; Ganschow, S.; Lassnig, A.; Gammer, C.; Todt, J.; Keckes, J.; Rettenwander, D. Understanding the Origin of Lithium Dendrite Branching in Li_{6.5}La₃Zr_{1.5}Ta_{0.5}O₁₂ Solid-State Electrolyte via Microscopy Measurements. *Nat. Commun.* **2024**, *15*, 8207. [[CrossRef](#)]
- Wang, Y.; Richards, W.D.; Ong, S.P.; Miara, L.J.; Kim, J.C.; Mo, Y.; Ceder, G. Design Principles for Solid-State Lithium Superionic Conductors. *Nat. Mater.* **2015**, *14*, 1026–1031. [[CrossRef](#)]
- Zhao, J.; Feng, X.; Pang, Q.; Fowler, M.; Lian, Y.; Ouyang, M.; Burke, A.F. Battery Safety: Machine Learning-Based Prognostics. *Prog. Energy Combust. Sci.* **2024**, *102*, 101142. [[CrossRef](#)]
- Misiani, A.N.; Oni, B.A. A Review on Challenges in Low Temperature Lithium-Ion Cells and Future Prospects. *Appl. Energy* **2025**, *393*, 125987. [[CrossRef](#)]

24. Reisecker, V.; Flatscher, F.; Porz, L.; Fincher, C.; Todt, J.; Hanghofer, I.; Hennige, V.; Linares-Moreau, M.; Falcaro, P.; Ganschow, S.; et al. Effect of Pulse-Current-Based Protocols on the Lithium Dendrite Formation and Evolution in All-Solid-State Batteries. *Nat. Commun.* **2023**, *14*, 2432. [[CrossRef](#)] [[PubMed](#)]
25. Du, H.; Wang, Y.; Kang, Y.; Zhao, Y.; Tian, Y.; Wang, X.; Tan, Y.; Liang, Z.; Wozny, J.; Li, T.; et al. Side Reactions/Changes in Lithium-Ion Batteries: Mechanisms and Strategies for Creating Safer and Better Batteries. *Adv. Mater.* **2024**, *36*, 2401482. [[CrossRef](#)]
26. Krauskopf, T.; Richter, F.H.; Zeier, W.G.; Janek, J. Physicochemical Concepts of the Lithium Metal Anode in Solid-State Batteries. *Chem. Rev.* **2020**, *120*, 7745–7794. [[CrossRef](#)]
27. Gao, Y.; Wang, D.; Li, Y.C.; Yu, Z.; Mallouk, T.E.; Wang, D. Salt-Based Organic–Inorganic Nanocomposites: Towards A Stable Lithium Metal/Li₁₀ GeP₂ S₁₂ Solid Electrolyte Interface. *Angew. Chem. Int. Ed.* **2018**, *57*, 13608–13612. [[CrossRef](#)]
28. Yao, M.; Shi, J.; Luo, A.; Zhang, Z.; Zhu, G.; Xu, H.; Xu, J.; Jiang, L.; Jiang, K. Advances in Sulfide Solid-State Electrolytes for Lithium Batteries. *Energy Storage Mater.* **2025**, *75*, 104018. [[CrossRef](#)]
29. Xu, C.; Chen, L.; Wu, F. Unveiling the Power of Sulfide Solid Electrolytes for Next-Generation All-Solid-State Lithium Batteries. *Next Mater.* **2025**, *6*, 100428. [[CrossRef](#)]
30. Man, B.; Zeng, Y.; Liu, Q.; Chen, Y.; Li, X.; Luo, W.; Zhang, Z.; He, C.; Jie, M.; Liu, S. A Comprehensive Review of Sulfide Solid-State Electrolytes: Properties, Synthesis, Applications, and Challenges. *Crystals* **2025**, *15*, 492. [[CrossRef](#)]
31. Apelt, S.; Höhne, S.; Mehner, E.; Böhm, C.; Malanin, M.; Eichhorn, K.; Jehnichen, D.; Uhlmann, P.; Bergmann, U. Poly (Vinylidene Fluoride-co-trifluoroethylene) Thin Films after Dip- and Spin-Coating. *Macromol. Mater. Eng.* **2022**, *307*, 2200296. [[CrossRef](#)]
32. Liu, S.; Zhou, L.; Han, J.; Wen, K.; Guan, S.; Xue, C.; Zhang, Z.; Xu, B.; Lin, Y.; Shen, Y.; et al. Super Long-Cycling All-Solid-State Battery with Thin Li₆ PS₅ Cl-Based Electrolyte. *Adv. Energy Mater.* **2022**, *12*, 2200660. [[CrossRef](#)]
33. Liu, M.; Hong, J.J.; Sebti, E.; Zhou, K.; Wang, S.; Feng, S.; Pennebaker, T.; Hui, Z.; Miao, Q.; Lu, E.; et al. Surface Molecular Engineering to Enable Processing of Sulfide Solid Electrolytes in Humid Ambient Air. *arXiv* **2024**, arXiv:2412.04633. [[CrossRef](#)] [[PubMed](#)]
34. Kwon, O.; Kim, S.Y.; Hwang, J.; Han, J.; Yu, S.; Yim, T.; Oh, S.H. Design Principles for Moisture-Tolerant Sulfide-Based Solid Electrolytes and Associated Effect on the Electrochemical Performance of All-Solid-State Battery. *J. Electrochem. Sci. Technol.* **2024**, *15*, 437–458. [[CrossRef](#)]
35. Umair, M.; Zhou, S.; Li, W.; Rana, H.T.H.; Yang, J.; Cheng, L.; Li, M.; Yu, S.; Wei, J. Oxide Solid Electrolytes in Solid-State Batteries. *Batter. Supercaps* **2024**, *8*, e202400667. [[CrossRef](#)]
36. Gonzalez Puente, P.M.; Song, S.; Cao, S.; Rannalter, L.Z.; Pan, Z.; Xiang, X.; Shen, Q.; Chen, F. Garnet-Type Solid Electrolyte: Advances of Ionic Transport Performance and Its Application in All-Solid-State Batteries. *J. Adv. Ceram.* **2021**, *10*, 933–972. [[CrossRef](#)]
37. Neises, J.; Scheld, W.S.; Seok, A.-R.; Lobe, S.; Finsterbusch, M.; Uhlenbruck, S.; Schmeichel, R.; Benson, N. Study of Thermal Material Properties for Ta- and Al-Substituted Li₇ La₃ Zr₂ O₁₂ (LLZO) Solid-State Electrolyte in Dependency of Temperature and Grain Size. *J. Mater. Chem. A* **2022**, *10*, 12177–12186. [[CrossRef](#)]
38. Ni, J.E.; Case, E.D.; Sakamoto, J.S.; Rangasamy, E.; Wolfenstine, J.B. Room Temperature Elastic Moduli and Vickers Hardness of Hot-Pressed LLZO Cubic Garnet. *J. Mater. Sci.* **2012**, *47*, 7978–7985. [[CrossRef](#)]
39. Wolfenstine, J.; Allen, J.L.; Sakamoto, J.; Siegel, D.J.; Choe, H. Mechanical Behavior of Li-Ion-Conducting Crystalline Oxide-Based Solid Electrolytes: A Brief Review. *Ionics* **2018**, *24*, 1271–1276. [[CrossRef](#)]
40. Ding, H.; Wang, M.; Shan, X.; Yang, G.; Tian, M. Advancements in Active Filler-Contained Polymer Solid-State Electrolytes for Lithium-Metal Batteries: A Concise Review. *Supramol. Mater.* **2025**, *4*, 100097. [[CrossRef](#)]
41. Irfan, M.; Yang, Z.; Su, J.; Zhang, W. Polymer-Based Solid-State Electrolytes. In *ACS Symposium Series*; Gupta, R.K., Ed.; American Chemical Society: Washington, DC, USA, 2022; Volume 1413, pp. 201–232. ISBN 978-0-8412-9768-5.
42. Lee, T.K.; Zaini, N.F.M.; Mobarak, N.N.; Hassan, N.H.; Noor, S.A.M.; Mamat, S.; Loh, K.S.; KuBulat, K.H.; Su'ait, M.S.; Ahmad, A. PEO Based Polymer Electrolyte Comprised of Epoxidized Natural Rubber Material (ENR50) for Li-Ion Polymer Battery Application. *Electrochim. Acta* **2019**, *316*, 283–291. [[CrossRef](#)]
43. Xue, Z.; He, D.; Xie, X. Poly (Ethylene Oxide)-Based Electrolytes for Lithium-Ion Batteries. *J. Mater. Chem. A* **2015**, *3*, 19218–19253. [[CrossRef](#)]
44. Appetecchi, G.B.; Hassoun, J.; Scrosati, B.; Croce, F.; Cassel, F.; Salomon, M. Hot-Pressed, Solvent-Free, Nanocomposite, PEO-Based Electrolyte Membranes. *J. Power Sources* **2003**, *124*, 246–253. [[CrossRef](#)]
45. Wu, Z.; Wang, Y.; Du, W.; Shen, K.; Chen, B.; Pan, H.; Wu, Y.; Lu, Y. Controlled Radical Polymerization-Derived Solid-State Polymer Electrolytes for Lithium Batteries. *EnergyChem* **2025**, *7*, 100160. [[CrossRef](#)]
46. Croce, F.; Appetecchi, G.B.; Persi, L.; Scrosati, B. Nanocomposite Polymer Electrolytes for Lithium Batteries. *Nature* **1998**, *394*, 456–458. [[CrossRef](#)]
47. Armand, M.; Tarascon, J.-M. Building Better Batteries. *Nature* **2008**, *451*, 652–657. [[CrossRef](#)] [[PubMed](#)]

48. Yoon, J.H.; Cho, W.-J.; Kang, T.H.; Lee, M.; Yi, G.-R. Nanostructured Polymer Electrolytes for Lithium-Ion Batteries. *Macromol. Res.* **2021**, *29*, 509–518. [[CrossRef](#)]
49. Luo, S.; Liu, X.; Gao, L.; Deng, N.; Sun, X.; Li, Y.; Zeng, Q.; Wang, H.; Cheng, B.; Kang, W. A Review on Modified Polymer Composite Electrolytes for Solid-State Lithium Batteries. *Sustain. Energy Fuels* **2022**, *6*, 5019–5044. [[CrossRef](#)]
50. Chae, W.; Kim, B.; Ryoo, W.S.; Earmme, T. A Brief Review of Gel Polymer Electrolytes Using In Situ Polymerization for Lithium-Ion Polymer Batteries. *Polymers* **2023**, *15*, 803. [[CrossRef](#)]
51. Chattopadhyay, J.; Pathak, T.S.; Santos, D.M.F. Applications of Polymer Electrolytes in Lithium-Ion Batteries: A Review. *Polymers* **2023**, *15*, 3907. [[CrossRef](#)]
52. Li, Y.; Canepa, P.; Gorai, P. Role of Electronic Passivation in Stabilizing the Lithium— $\text{Li}_x\text{PO}_y\text{N}_z$ Solid-Electrolyte Interphase. *PRX Energy* **2022**, *1*, 023004. [[CrossRef](#)]
53. Cao, D.; Sun, X.; Li, Q.; Natan, A.; Xiang, P.; Zhu, H. Lithium Dendrite in All-Solid-State Batteries: Growth Mechanisms, Suppression Strategies, and Characterizations. *Matter* **2020**, *3*, 57–94. [[CrossRef](#)]
54. Cheng, D.; Wynn, T.A.; Wang, X.; Wang, S.; Zhang, M.; Shimizu, R.; Bai, S.; Nguyen, H.; Fang, C.; Kim, M.; et al. Unveiling the Stable Nature of the Solid Electrolyte Interphase between Lithium Metal and LiPON via Cryogenic Electron Microscopy. *arXiv* **2020**, arXiv:2006.12764. [[CrossRef](#)]
55. LaCoste, J.; Li, Z.; Xu, Y.; He, Z.; Matherne, D.; Zakutayev, A.; Fei, L. Investigating the Effects of Lithium Phosphorous Oxynitride Coating on Blended Solid Polymer Electrolytes. *ACS Appl. Mater. Interfaces* **2020**, *12*, 40749–40758. [[CrossRef](#)] [[PubMed](#)]
56. Klorman, J.A.; Guo, Q.; Lau, K.C. First-Principles Study of Amorphous Al_2O_3 ALD Coating in Li-S Battery Electrode Design. *Energies* **2022**, *15*, 390. [[CrossRef](#)]
57. Zhou, H.; Yu, S.; Liu, H.; Liu, P. Protective Coatings for Lithium Metal Anodes: Recent Progress and Future Perspectives. *J. Power Sources* **2020**, *450*, 227632. [[CrossRef](#)]
58. Lee, S.; Lee, K.; Kim, S.; Yoon, K.; Han, S.; Lee, M.H.; Ko, Y.; Noh, J.H.; Kim, W.; Kang, K. Design of a Lithiophilic and Electron-Blocking Interlayer for Dendrite-Free Lithium-Metal Solid-State Batteries. *Sci. Adv.* **2022**, *8*, eabq0153. [[CrossRef](#)]
59. Pang, B.; Wu, Z.; Zhang, W.; Huang, H.; Gan, Y.; Xia, Y.; He, X.; Xia, X.; Zhang, J. Ag Nanoparticles Incorporated Interlayer Enables Ultrahigh Critical Current Density for $\text{Li}_6\text{PS}_5\text{Cl}$ -Based All-Solid-State Lithium Batteries. *J. Power Sources* **2023**, *563*, 232836. [[CrossRef](#)]
60. Wan, J.; Liu, X.; Diemant, T.; Wan, M.; Passerini, S.; Paillard, E. Single-Ion Conducting Interlayers for Improved Lithium Metal Plating. *Energy Storage Mater.* **2023**, *63*, 103029. [[CrossRef](#)]
61. Hoang, B.; Damircheli, R.; Ferrari, V.C.; Stewart, D.M.; Brausch, M.; Nguyen, N.; Lin, C.-F. Highly Effective Polyacrylonitrile-Rich Artificial Solid-Electrolyte-Interphase for Dendrite-Free Li-Metal/Solid-State Battery. *ACS Appl. Mater. Interfaces* **2024**, *16*, 63703–63712. [[CrossRef](#)]
62. Ci, N.; Zhang, L.; Li, J.; Li, D.; Cheng, J.; Sun, Q.; Xi, Z.; Xu, Z.; Zhao, G.; Ci, L. In Situ Construction of a Flexible Interlayer for Durable Solid-State Lithium Metal Batteries. *Carbon* **2022**, *187*, 13–21. [[CrossRef](#)]
63. Ren, P.; Wang, X.; Huang, B.; Liu, Z.; Liu, R. Li_3N Interlayer Enables Stable Long-Term Cycling for Sulfide-Based All-Solid-State Li Metal Batteries. *J. Energy Storage* **2024**, *82*, 110200. [[CrossRef](#)]
64. You, X.; Chen, N.; Xie, G.; Xu, S.; Buriaik, J.; Sang, L. Dual-Component Interlayer Enables Uniform Lithium Deposition and Dendrite Suppression for Solid-State Batteries. *ACS Appl. Mater. Interfaces* **2024**, *16*, 35761–35770. [[CrossRef](#)] [[PubMed](#)]
65. Dong, G.; Dong, N.; Liu, B.; Tian, G.; Qi, S.; Wu, D. Ultrathin Inorganic-Nanoshell Encapsulation: TiO_2 Coated Polyimide Nanofiber Membrane Enabled by Layer-by-Layer Deposition for Advanced and Safe High-Power LIB Separator. *J. Membr. Sci.* **2020**, *601*, 117884. [[CrossRef](#)]
66. Sang, J.; Tang, B.; Pan, K.; He, Y.-B.; Zhou, Z. Current Status and Enhancement Strategies for All-Solid-State Lithium Batteries. *Acc. Mater. Res.* **2023**, *4*, 472–483. [[CrossRef](#)]
67. Zhang, Y.; Wang, J. Stabilizing the Cathode-Electrolyte Interphase for Superior Li-Ion Batteries. *Green Chem. Eng.* **2025**, *in press* S2666952825000470. [[CrossRef](#)]
68. Nogales, P.M.; Lee, S.; Yang, S.; Yang, I.; Choi, S.H.; Park, S.-M.; Lee, J.H.; Kim, C.J.; An, J.-C.; Jeong, S.-K. Stabilizing the Solid Electrolyte Interphase of SiO_x Negative Electrodes: The Role of Fluoroethylene Carbonate in Enhancing Electrochemical Performance. *Batteries* **2024**, *10*, 385. [[CrossRef](#)]
69. Park, S.K.; Copic, D.; Zhao, T.Z.; Rutkowska, A.; Wen, B.; Sanders, K.; He, R.; Kim, H.-K.; De Volder, M. 3D Porous Cu-Composites for Stable Li-Metal Battery Anodes. *ACS Nano* **2023**, *17*, 14658–14666. [[CrossRef](#)]
70. Sastre, J.; Futscher, M.H.; Pompizi, L.; Aribia, A.; Priebe, A.; Overbeck, J.; Stiefel, M.; Tiwari, A.N.; Romanyuk, Y.E. Blocking Lithium Dendrite Growth in Solid-State Batteries with an Ultrathin Amorphous Li-La-Zr-O Solid Electrolyte. *Commun. Mater.* **2021**, *2*, 76. [[CrossRef](#)]
71. Zhang, Y.; Tang, Z.; Mei, Y.; Xiao, Y.; Xiang, X.; Luo, D.; Deng, J. Study on the Electrochemical Performance of All-Solid-State Lithium Battery Based on Li_3BO_3 Gradient Coated LiCoO_2 Cathode. *Appl. Surf. Sci.* **2023**, *630*, 157488. [[CrossRef](#)]

72. Du, C.; Li, Z.; Fang, Z.; Fang, X.; Ji, X.; Zhao, Z.; Liu, D.; Li, R.; Xiang, X.; Yang, H. Constructing a Three-Dimensional Continuous Grain Boundary with Lithium Ion Conductivity and Electron Blocking Property in LLZO to Suppress Lithium Dendrites. *J. Alloys Compd.* **2024**, *1003*, 175769. [[CrossRef](#)]
73. Huang, J.; Li, C.; Jiang, D.; Gao, J.; Cheng, L.; Li, G.; Luo, H.; Xu, Z.; Shin, D.; Wang, Y.; et al. Solid-State Electrolytes for Lithium Metal Batteries: State-of-the-Art and Perspectives. *Adv. Funct. Mater.* **2025**, *35*, 2411171. [[CrossRef](#)]
74. Pervez, S.A.; Madinehei, M.; Moghimian, N. Graphene in Solid-State Batteries: An Overview. *Nanomaterials* **2022**, *12*, 2310. [[CrossRef](#)] [[PubMed](#)]
75. Yang, T.; Zheng, J.; Cheng, Q.; Hu, Y.-Y.; Chan, C.K. Composite Polymer Electrolytes with $\text{Li}_7\text{La}_3\text{Zr}_2\text{O}_{12}$ Garnet-Type Nanowires as Ceramic Fillers: Mechanism of Conductivity Enhancement and Role of Doping and Morphology. *ACS Appl. Mater. Interfaces* **2017**, *9*, 21773–21780. [[CrossRef](#)] [[PubMed](#)]
76. Zhang, Y.; Bao, W.; Hu, Z.; Wang, Y.; Jiang, J.; Huo, S.; Fan, W.; Chen, W.; Jing, X.; Long, X. Poly (Ionic Liquid)-Functionalized Graphene Oxide Towards Ambient Temperature Operation of All-Solid-State Peo-Based Polymer Electrolyte Lithium Metal Batteries. *Chem. Eng. J.* **2022**, *437*, 135420. [[CrossRef](#)]
77. Otabil, A.; Kharbatli, A.-R.; Siddique, S.K.; Liao, K.; Schiffer, A. Recent Developments in the Incorporation of 1D/2D Nanofillers in Polymer Derived Ceramics—A Review. *Adv. Compos. Hybrid. Mater.* **2025**, *8*, 267. [[CrossRef](#)]
78. Athanasiou, C.E.; Jin, M.Y.; Ramirez, C.; Padture, N.P.; Sheldon, B.W. High-Toughness Inorganic Solid Electrolytes via the Use of Reduced Graphene Oxide. *Matter* **2020**, *3*, 212–229. [[CrossRef](#)]
79. Safian, M.T.; Umar, K.; Ibrahim, M.N.M. Synthesis and Scalability of Graphene and Its Derivatives: A Journey towards Sustainable and Commercial Material. *J. Clean. Prod.* **2021**, *318*, 128603. [[CrossRef](#)]
80. Soldano, C.; Mahmood, A.; Dujardin, E. Production, Properties and Potential of Graphene. *Carbon* **2010**, *48*, 2127–2150. [[CrossRef](#)]
81. Cha, E.; Kim, D.K.; Choi, W. Advances of 2D MoS₂ for High-Energy Lithium Metal Batteries. *Front. Energy Res.* **2021**, *9*, 645403. [[CrossRef](#)]
82. Fu, J.; Yu, P.; Zhang, N.; Ren, G.; Zheng, S.; Huang, W.; Long, X.; Li, H.; Liu, X. In Situ Formation of a Bifunctional Interlayer Enabled by a Conversion Reaction to Initiatively Prevent Lithium Dendrites in a Garnet Solid Electrolyte. *Energy Environ. Sci.* **2019**, *12*, 1404–1412. [[CrossRef](#)]
83. He, Y.; Wang, C.; Zhang, R.; Zou, P.; Chen, Z.; Bak, S.-M.; Trask, S.E.; Du, Y.; Lin, R.; Hu, E.; et al. A Self-Healing Plastic Ceramic Electrolyte by an Aprotic Dynamic Polymer Network for Lithium Metal Batteries. *Nat. Commun.* **2024**, *15*, 10015. [[CrossRef](#)]
84. Chen, J.; Gao, Y.; Shi, L.; Yu, W.; Sun, Z.; Zhou, Y.; Liu, S.; Mao, H.; Zhang, D.; Lu, T.; et al. Phase-Locked Constructing Dynamic Supramolecular Ionic Conductive Elastomers with Superior Toughness, Autonomous Self-Healing and Recyclability. *Nat. Commun.* **2022**, *13*, 4868. [[CrossRef](#)]
85. Liu, F.-Q.; Wang, W.-P.; Yin, Y.-X.; Zhang, S.-F.; Shi, J.-L.; Wang, L.; Zhang, X.-D.; Zheng, Y.; Zhou, J.-J.; Li, L.; et al. Upgrading Traditional Liquid Electrolyte via in Situ Gelation for Future Lithium Metal Batteries. *Sci. Adv.* **2018**, *4*, eaat5383. [[CrossRef](#)]
86. Le Mong, A.; Kim, D. Self-Healable, Super Li-Ion Conductive, and Flexible Quasi-Solid Electrolyte for Long-Term Safe Lithium Sulfur Batteries. *J. Mater. Chem. A* **2023**, *11*, 6503–6521. [[CrossRef](#)]
87. He, Y.; Wang, C.; Lin, R.; Hu, E.; Trask, S.E.; Li, J.; Xin, H.L. A Self-Healing, Flowable, Yet Solid Electrolyte Suppresses Li-Metal Morphological Instabilities. *Adv. Mater.* **2024**, *36*, 2406315. [[CrossRef](#)] [[PubMed](#)]
88. Zhang, X.; Zhao, H.; Wang, N.; Xiao, Y.; Liang, S.; Yang, J.; Huang, X. Gradual Gradient Distribution Composite Solid Electrolyte for Solid-State Lithium Metal Batteries with Ameliorated Electrochemical Performance. *J. Colloid Interface Sci.* **2024**, *658*, 836–845. [[CrossRef](#)] [[PubMed](#)]
89. Afauyl, R.A.P.; Habibi, M.F.; Budiman, B.A. Review on Manufacturing Methods of Functionally Graded Material of Solid-State Batteries. In Proceedings of the 2021 3rd International Symposium on Material and Electrical Engineering Conference (ISMEE), Bandung, Indonesia, 10–11 November 2021; pp. 236–241.
90. Deng, J.; Ren, X.; Lin, H.; Hu, L.; Bai, Y.; Yu, X.; Mo, J.; Zhang, Q.; Kang, F.; Li, B. Functionally Gradient Materials for Sustainable and High-Energy Rechargeable Lithium Batteries: Design Principles, Progress, and Perspectives. *J. Energy Chem.* **2024**, *99*, 426–449. [[CrossRef](#)]
91. Kim, J.; Lee, J.; Yun, J.; Choi, S.H.; Han, S.A.; Moon, J.; Kim, J.H.; Lee, J.; Park, M. Functionality of Dual-Phase Lithium Storage in a Porous Carbon Host for Lithium-Metal Anode. *Adv. Funct. Materials* **2020**, *30*, 1910538. [[CrossRef](#)]
92. Chen, L.; Liu, H.; Li, M.; Zhou, S.; Mo, F.; Yu, S.; Wei, J. Boosting the Performance of Lithium Metal Anodes with Three-Dimensional Lithium Hosts: Recent Progress and Future Perspectives. *Batteries* **2023**, *9*, 391. [[CrossRef](#)]
93. Pathak, R.; Chen, K.; Wu, F.; Mane, A.U.; Bugga, R.V.; Elam, J.W.; Qiao, Q.; Zhou, Y. Advanced Strategies for the Development of Porous Carbon as a Li Host/Current Collector for Lithium Metal Batteries. *Energy Storage Mater.* **2021**, *41*, 448–465. [[CrossRef](#)]
94. Zhang, Y.; Liu, B.; Hitz, E.; Luo, W.; Yao, Y.; Li, Y.; Dai, J.; Chen, C.; Wang, Y.; Yang, C.; et al. A Carbon-Based 3D Current Collector with Surface Protection for Li Metal Anode. *Nano Res.* **2017**, *10*, 1356–1365. [[CrossRef](#)]
95. Xu, Q.; Yang, X.; Rao, M.; Lin, D.; Yan, K.; Du, R.; Xu, J.; Zhang, Y.; Ye, D.; Yang, S.; et al. High Energy Density Lithium Metal Batteries Enabled by a Porous Graphene/MgF₂ Framework. *Energy Storage Mater.* **2020**, *26*, 73–82. [[CrossRef](#)]

96. Lee, J.; Won, E.-S.; Kim, D.-M.; Kim, H.; Kwon, B.; Park, K.; Jo, S.; Lee, S.; Lee, J.-W.; Lee, K.T. Three-Dimensional Porous Frameworks for Li Metal Batteries: Superconformal versus Conformal Li Growth. *ACS Appl. Mater. Interfaces* **2021**, *13*, 33056–33065. [CrossRef] [PubMed]
97. Zhao, X.; Xia, S.; Zhang, X.; Pang, Y.; Xu, F.; Yang, J.; Sun, L.; Zheng, S. Highly Lithiophilic Copper-Reinforced Scaffold Enables Stable Li Metal Anode. *ACS Appl. Mater. Interfaces* **2021**, *13*, 20240–20250. [CrossRef]
98. Chen, H.; Pei, A.; Wan, J.; Lin, D.; Vilá, R.; Wang, H.; Mackanic, D.; Steinrück, H.-G.; Huang, W.; Li, Y.; et al. Tortuosity Effects in Lithium-Metal Host Anodes. *Joule* **2020**, *4*, 938–952. [CrossRef]
99. Yan, X.; Lin, L.; Chen, Q.; Xie, Q.; Qu, B.; Wang, L.; Peng, D. Multifunctional Roles of Carbon-based Hosts for Li-metal Anodes: A Review. *Carbon Energy* **2021**, *3*, 303–329. [CrossRef]
100. Nkosi, F.P.; Valvo, M.; Mindemark, J.; Dzulkurnain, N.A.; Hernández, G.; Mahun, A.; Abbrent, S.; Brus, J.; Kobera, L.; Edström, K. Garnet-Poly (ϵ -Caprolactone-Co-Trimethylene Carbonate) Polymer-in-Ceramic Composite Electrolyte for All-Solid-State Lithium-Ion Batteries. *ACS Appl. Energy Mater.* **2021**, *4*, 2531–2542. [CrossRef]
101. Rizvi, S.; Aladhyani, I.; Ding, Y.; Zhang, Q. Recent Advances in Doping $\text{Na}_3\text{Zr}_2\text{Si}_2\text{PO}_{12}$ (NASICON) Solid-State Electrolyte for Sodium-Ion Batteries. *Nano Energy* **2024**, *129*, 110009. [CrossRef]
102. Sayed, S.Y.; Reese, C.; Kim, Y.; Sachdev, A.K. 3D Current Collectors for Lithium Metal Anodes: A Review on Concepts of Performance. *Int. Mater. Rev.* **2025**, *70*, 139–204. [CrossRef]
103. Vilá, R.A.; Boyle, D.T.; Dai, A.; Zhang, W.; Sayavong, P.; Ye, Y.; Yang, Y.; Dionne, J.A.; Cui, Y. LiH Formation and Its Impact on Li Batteries Revealed by Cryogenic Electron Microscopy. *Sci. Adv.* **2023**, *9*, eadf3609. [CrossRef] [PubMed]
104. Gao, H.; Ai, X.; Wang, H.; Li, W.; Wei, P.; Cheng, Y.; Gui, S.; Yang, H.; Yang, Y.; Wang, M.-S. Visualizing the Failure of Solid Electrolyte under GPa-Level Interface Stress Induced by Lithium Eruption. *Nat. Commun.* **2022**, *13*, 5050. [CrossRef] [PubMed]
105. Zhao, L.; Feng, M.; Wu, C.; Guo, L.; Chen, Z.; Risal, S.; Ai, Q.; Lou, J.; Fan, Z.; Qi, Y.; et al. Imaging the Evolution of Lithium-Solid Electrolyte Interface Using Operando Scanning Electron Microscopy. *Nat. Commun.* **2025**, *16*, 4283. [CrossRef] [PubMed]
106. Zhang, L.; Yang, T.; Du, C.; Liu, Q.; Tang, Y.; Zhao, J.; Wang, B.; Chen, T.; Sun, Y.; Jia, P.; et al. Lithium Whisker Growth and Stress Generation in an in Situ Atomic Force Microscope–Environmental Transmission Electron Microscope Set-Up. *Nat. Nanotechnol.* **2020**, *15*, 94–98. [CrossRef]
107. Zaccarine, S. In-Situ XPS: Investigating Stable Interfaces for Improved Solid-State Battery Performance. Available online: <https://www.phi.com/news-and-articles/insitu-battery-spotlight.html> (accessed on 22 June 2025).
108. Huo, H.; Jiang, M.; Mogwitz, B.; Sann, J.; Yusim, Y.; Zuo, T.; Moryson, Y.; Minnmann, P.; Richter, F.H.; Veer Singh, C.; et al. Interface Design Enabling Stable Polymer/Thiophosphate Electrolyte Separators for Dendrite-Free Lithium Metal Batteries. *Angew. Chem. Int. Ed.* **2023**, *62*, e202218044. [CrossRef]
109. Zhu, C.; Fuchs, T.; Weber, S.A.L.; Richter, F.H.; Glasser, G.; Weber, F.; Butt, H.-J.; Janek, J.; Berger, R. Understanding the Evolution of Lithium Dendrites at $\text{Li}_{6.25}\text{Al}_{0.25}\text{La}_3\text{Zr}_2\text{O}_{12}$ Grain Boundaries via Operando Microscopy Techniques. *Nat. Commun.* **2023**, *14*, 1300. [CrossRef]
110. Lu, Y.; Zhao, C.-Z.; Hu, J.-K.; Sun, S.; Yuan, H.; Fu, Z.-H.; Chen, X.; Huang, J.-Q.; Ouyang, M.; Zhang, Q. The Void Formation Behaviors in Working Solid-State Li Metal Batteries. *Sci. Adv.* **2022**, *8*, eadd0510. [CrossRef]
111. Thomas, C.; Zhang, W.; Chancey, M.R.; Di Michiel, M.; Garman, K.; Wang, Y.; Harris, S.; Finegan, D.P.; Wang, Y.; Ban, C. Stress engineering for crack and dendrite prevention in solid electrolytes via ion implantation. *Cell Rep. Phys. Sci.* **2025**, *6*, 102544. [CrossRef]
112. Hu, J.; Sun, Z.; Gao, Y.; Li, P.; Wu, Y.; Chen, S.; Wang, R.; Li, N.; Yang, W.; Shen, Y.; et al. 3D Stress Mapping Reveals the Origin of Lithium-Deposition Heterogeneity in Solid-State Lithium-Metal Batteries. *Cell Rep. Phys. Sci.* **2022**, *3*, 100938. [CrossRef]
113. Sun, H.; Celadon, A.; Cloutier, S.G.; Al-Haddad, K.; Sun, S.; Zhang, G. Lithium Dendrites in All-solid-state Batteries: From Formation to Suppression. *Battery Energy* **2024**, *3*, 20230062. [CrossRef]
114. Maity, A.; Svirinovsky-Arbeli, A.; Buganim, Y.; Oppenheim, C.; Leskes, M. Tracking Dendrites and Solid Electrolyte Interphase Formation with Dynamic Nuclear Polarization—NMR Spectroscopy. *Nat. Commun.* **2024**, *15*, 9956. [CrossRef]
115. Liang, Z.; Xiang, Y.; Wang, K.; Zhu, J.; Jin, Y.; Wang, H.; Zheng, B.; Chen, Z.; Tao, M.; Liu, X.; et al. Understanding the Failure Process of Sulfide-Based All-Solid-State Lithium Batteries via Operando Nuclear Magnetic Resonance Spectroscopy. *Nat. Commun.* **2023**, *14*, 259. [CrossRef]
116. Jena, A.; Tong, Z.; Bazri, B.; Iputera, K.; Chang, H.; Hu, S.-F.; Liu, R.-S. In Situ/Operando Methods of Characterizing All-Solid-State Li-Ion Batteries: Understanding Li-Ion Transport during Cycle. *J. Phys. Chem. C* **2021**, *125*, 16921–16937. [CrossRef]
117. Banerjee, A.; Wang, X.; Fang, C.; Wu, E.A.; Meng, Y.S. Interfaces and Interphases in All-Solid-State Batteries with Inorganic Solid Electrolytes. *Chem. Rev.* **2020**, *120*, 6878–6933. [CrossRef]
118. Wenzel, S.; Weber, D.A.; Leichtweiss, T.; Busche, M.R.; Sann, J.; Janek, J. Interphase Formation and Degradation of Charge Transfer Kinetics between a Lithium Metal Anode and Highly Crystalline $\text{Li}_7\text{P}_3\text{S}_{11}$ Solid Electrolyte. *Solid State Ion.* **2016**, *286*, 24–33. [CrossRef]

119. Cheng, Q.; Wei, L.; Liu, Z.; Ni, N.; Sang, Z.; Zhu, B.; Xu, W.; Chen, M.; Miao, Y.; Chen, L.-Q.; et al. Operando and Three-Dimensional Visualization of Anion Depletion and Lithium Growth by Stimulated Raman Scattering Microscopy. *Nat. Commun.* **2018**, *9*, 2942. [[CrossRef](#)]
120. Talian, S.D.; Kapun, G.; Moškon, J.; Dominko, R.; Gaberšček, M. Operando Impedance Spectroscopy with Combined Dynamic Measurements and Overvoltage Analysis in Lithium Metal Batteries. *Nat. Commun.* **2025**, *16*, 2030. [[CrossRef](#)] [[PubMed](#)]
121. Li, Z.; Fu, J.; Guo, X. How to Commercialize Solid-State Batteries: A Perspective from Solid Electrolytes. *Natl. Sci. Open* **2023**, *2*, 20220036. [[CrossRef](#)]
122. Wan, H.; Wang, Z.; Liu, S.; Zhang, B.; He, X.; Zhang, W.; Wang, C. Critical Interphase Overpotential as a Lithium Dendrite-Suppression Criterion for All-Solid-State Lithium Battery Design. *Nat. Energy* **2023**, *8*, 473–481. [[CrossRef](#)]
123. Kato, Y.; Hori, S.; Kanno, R. $\text{Li}_{10}\text{GeP}_2\text{S}_{12}$ —Type Superionic Conductors: Synthesis, Structure, and Ionic Transportation. *Adv. Energy Mater.* **2020**, *10*, 2002153. [[CrossRef](#)]
124. Yuan, C.; Sheldon, B.W.; Xu, J. Heterogeneous Reinforcements to Mitigate Li Penetration through Solid Electrolytes in All-Solid-State Batteries. *Adv. Energy Mater.* **2022**, *12*, 2201804. [[CrossRef](#)]
125. Hu, B.; Zhang, S.; Ning, Z.; Spencer-Jolly, D.; Melvin, D.L.R.; Gao, X.; Perera, J.; Pu, S.D.; Rees, G.J.; Wang, L.; et al. Deflecting Lithium Dendritic Cracks in Multi-Layered Solid Electrolytes. *Joule* **2024**, *8*, 2623–2638. [[CrossRef](#)]
126. Ning, Z.; Li, G.; Melvin, D.L.R.; Chen, Y.; Bu, J.; Spencer-Jolly, D.; Liu, J.; Hu, B.; Gao, X.; Perera, J.; et al. Dendrite Initiation and Propagation in Lithium Metal Solid-State Batteries. *Nature* **2023**, *618*, 287–293. [[CrossRef](#)]
127. Wang, Z.-X.; Lu, Y.; Zhao, C.-Z.; Huang, W.-Z.; Huang, X.-Y.; Kong, W.-J.; Li, L.-X.; Wang, Z.-Y.; Yuan, H.; Huang, J.-Q.; et al. Suppressing Li Voids in All-Solid-State Lithium Metal Batteries through Li Diffusion Regulation. *Joule* **2024**, *8*, 2794–2810. [[CrossRef](#)]
128. Tao, J.; Chen, Y.; Bhardwaj, A.; Wen, L.; Li, J.; Kolosov, O.V.; Lin, Y.; Hong, Z.; Huang, Z.; Mathur, S. Combating Li Metal Deposits in All-Solid-State Battery via the Piezoelectric and Ferroelectric Effects. *Proc. Natl. Acad. Sci. USA* **2022**, *119*, e2211059119. [[CrossRef](#)] [[PubMed](#)]
129. Shan, J.; Gu, R.; Xu, J.; Gong, S.; Guo, S.; Xu, Q.; Shi, P.; Min, Y. Heterojunction Ferroelectric Materials Enhance Ion Transport and Fast Charging of Polymer Solid Electrolytes for Lithium Metal Batteries. *Adv. Energy Mater.* **2025**, *15*, 2405220. [[CrossRef](#)]
130. Sung, J.; Heo, J.; Kim, D.-H.; Jo, S.; Ha, Y.-C.; Kim, D.; Ahn, S.; Park, J.-W. Recent Advances in All-Solid-State Batteries for Commercialization. *Mater. Chem. Front.* **2024**, *8*, 1861–1887. [[CrossRef](#)]
131. Avadanii, D.; Ganschow, S.; Stypa, M.; Müller, S.; Lang, S.; Kramer, D.; Kirchlechner, C.; Mönig, R. Disconnected Lithium Metal Damages Solid-State Electrolytes. *ACS Energy Lett.* **2025**, *10*, 2061–2067. [[CrossRef](#)]
132. Antony Jose, S.; Gallant, A.; Gomez, P.L.; Jagers, Z.; Johansson, E.; LaPierre, Z.; Menezes, P.L. Solid-State Lithium Batteries: Advances, Challenges, and Future Perspectives. *Batteries* **2025**, *11*, 90. [[CrossRef](#)]
133. Nikodimos, Y.; Huang, C.-J.; Taklu, B.W.; Su, W.-N.; Hwang, B.J. Chemical Stability of Sulfide Solid-State Electrolytes: Stability toward Humid Air and Compatibility with Solvents and Binders. *Energy Environ. Sci.* **2022**, *15*, 991–1033. [[CrossRef](#)]

Disclaimer/Publisher’s Note: The statements, opinions and data contained in all publications are solely those of the individual author(s) and contributor(s) and not of MDPI and/or the editor(s). MDPI and/or the editor(s) disclaim responsibility for any injury to people or property resulting from any ideas, methods, instructions or products referred to in the content.